Table S20 is corrected in this file. In the original version of the SI Appendix, the second and last second columns of this table were not wide enough, and as a consequence some entries got truncated.

SI APPENDIX

SUPPLEMENTARY INFORMATION

AUGUST 9, 2018

Revised M06 Density Functional for Main-Group and Transition-Metal Chemistry

Ying Wang[1,#], Pragya Verma[2,#], Xinsheng Jin[1], Donald G. Truhlar[2,]* and Xiao He[1,3,]*

[1]*School of Chemistry and Molecular Engineering, State Key Laboratory of Precision Spectroscopy, and Shanghai Engineering Research Center of Molecular Therapeutics and New Drug Development, East China Normal University, Shanghai, 200062, China*

[2]*Department of Chemistry, Chemical Theory Center, Nanoporous Materials Genome Center, and Minnesota Supercomputing Institute, University of Minnesota, Minneapolis, Minnesota, 55455-0431, USA*

[3]*NYU-ECNU Center for Computational Chemistry at NYU Shanghai, Shanghai, 200062, China*

[#]These authors contribute equally to this work.

*Corresponding authors. Email: xiaohe@phy.ecnu.edu.cn (X.H.) and truhlar@umn.edu (D.G.T.)

Contents

www.pnas.org/cgi/doi/10.1073/pnas.1810421115

1. Methods

1.1 Design and parameterization for the revM06 functional

The energy functional for the revM06 functional is

$$E_{XC}^{\mathrm{revM06}} = \frac{X}{100} E_X^{\mathrm{HF}} + E_X^{\mathrm{revM06-L}} + E_C^{\mathrm{revM06-L}} \quad \text{(S1)}$$

where E_X^{HF} is the nonlocal Hartree–Fock (HF) exchange energy, X is the percentage of Hartree–Fock exchange, and $E_X^{\mathrm{revM06-L}}$ and $E_C^{\mathrm{revM06-L}}$ are respectively local exchange and correlation terms based on the revM06-L functional form.(1) We optimized the coefficient X together with the parameters in $E_X^{\mathrm{revM06-L}}$ and $E_C^{\mathrm{revM06-L}}$.The local exchange is a combination of the VSXC(2) and M05(3) exchange functional forms; and the revM06 correlation functional E_C^{revM06} is also a combination of the M05 and VSXC correlation functional forms, which include both opposite-spin correlation energy $E_C^{\alpha\beta}$ and parallel-spin correlation energy $E_C^{\sigma\sigma}$.

The local exchange part of the revM06 functional is given by,

$$E_X^{\mathrm{revM06-L}} = \sum_\sigma \int dr \left[F_{X_\sigma}^{\mathrm{PBE}}(\rho_\sigma, \nabla\rho_\sigma) f(\omega_\sigma) + \varepsilon_{X_\sigma}^{\mathrm{LSDA}} h_X(x_\sigma, z_\sigma) \right] \quad \text{(S2)}$$

where $\rho_\sigma, \nabla\rho_\sigma$ are the spin density and its gradient, respectively; $h_X(x_\sigma, Z_\sigma)$ is based on the VSXC(2) functional,

$$h_X(x_\sigma, Z_\sigma) = \left(\frac{d_0}{\gamma(x_\sigma, z_\sigma)} + \frac{d_1 x_\sigma^2 + d_2 z_\sigma}{\gamma_\sigma^2(x_\sigma, z_\sigma)} + \frac{d_3 x_\sigma^4 + d_4 x_\sigma^2 z_\sigma + d_5 z_\sigma^2}{\gamma_\sigma^3(x_\sigma, z_\sigma)} \right) \quad \text{(S3)}$$

and

$$\gamma(x_\sigma, Z_\sigma) = 1 + \alpha(x_\sigma^2 + z_\sigma) \quad \text{(S4)}$$

in which the reduced spin density gradient x_σ and the working variable Z_σ are defined by,

$$x_\sigma = \frac{|\nabla\rho_\sigma|}{\rho_\sigma^{4/3}}, \ \sigma = \alpha, \beta \quad \text{(S5)}$$

$$z_\sigma = \frac{2\tau_\sigma}{\rho_\sigma^{5/3}} - \frac{3}{5}(6\pi^2)^{\frac{2}{3}} \quad \text{(S6)}$$

and τ_σ is the spin-specific kinetic energy density given by,

$$\tau_\sigma = \frac{1}{2}\sum_{i=1}^{n_\sigma} |\nabla\psi_{i\sigma}(\mathbf{r})|^2 \quad \text{(S7)}$$

where $\psi_{i\sigma}$ is the spatial part of an occupied Kohn-Sham spin-orbital, and n_σ is the number of occupied spin-orbitals of spin σ. Furthermore, $F_{X_\sigma}^{\mathrm{PBE}}$ is the exchange energy density of the Perdew-Burke-Ernzerhof (PBE) exchange functional(4), $\varepsilon_{\mathrm{X}_\sigma}^{\mathrm{LSDA}}$ is the Gàspàr–Kohn–Sham local spin density approximation (LSDA) for the exchange energy,

$$\varepsilon_{X_\sigma}^{\mathrm{LSDA}} = -\frac{3}{2}\left(\frac{3}{4\pi}\right)^{\frac{1}{3}}\rho_\sigma^{\frac{4}{3}} \tag{S8}$$

and $f(w_\sigma)$ is the spin kinetic-energy-density enhancement factor,

$$f(w_\sigma) = \sum_{i=0}^{11} a_i \omega_\sigma^i \tag{S9}$$

where the variable ω_σ is a function of t_σ, which is a function of the spin density ρ_σ and spin kinetic energy density τ_σ,

$$\omega_\sigma = \frac{t_\sigma - 1}{t_\sigma + 1} \tag{S10}$$

$$t_\sigma = \frac{3(6\pi^2)^{\frac{2}{3}}\rho_\sigma^{\frac{5}{3}}}{10\tau_\sigma} \tag{S11}$$

The opposite-spin correlation energy of the revM06-L and revM06 functionals is defined as,

$$E_{\mathrm{C}}^{\alpha\beta} = \int e_{\alpha\beta}^{\mathrm{UEG}}\left[g_{\alpha\beta}(x_\alpha, x_\beta) + h_{\alpha\beta}(x_{\alpha\beta}, z_{\alpha\beta})\right]dr \tag{S12}$$

in which

$$g_{\alpha\beta}(x_\alpha, x_\beta) = \sum_{i=0}^{4} c_{C_{\alpha\beta,i}}\left(\frac{\gamma_{C_{\alpha\beta}}(x_\alpha^2 + x_\beta^2)}{1 + \gamma_{C_{\alpha\beta}}(x_\alpha^2 + x_\beta^2)}\right)^i \tag{S13}$$

and $h_{\alpha\beta}$ is defined in Eq. (S3).

The parallel spin correlation energy of the revM06-L and revM06 functionals is given by,

$$E_{\mathrm{C}}^{\sigma\sigma} = \int e_{\sigma\sigma}^{\mathrm{UEG}}\left[g_{\sigma\sigma}(x_\sigma) + h_{\sigma\sigma}(x_\sigma, z_\sigma)\right]D_\sigma dr \tag{S14}$$

where

$$g_{\sigma\sigma}(x_\sigma) = \sum_{i=0}^{4} c_{C_{\sigma\sigma,i}}\left(\frac{\gamma_{C_{\sigma\sigma}} x_\sigma^2}{1 + \gamma_{C_{\sigma\sigma}} x_\sigma^2}\right)^i \tag{S15}$$

and $h_{\sigma\sigma}$ is also defined in Eq. (S3); D_σ is the self-interaction correlation factor

$$D_\sigma = 1 - \frac{\tau^W}{\tau_\sigma} \tag{S16}$$

where τ^W is the von Weizsäcker kinetic energy density:

$$\tau^W = \frac{|\nabla\rho_\sigma|^2}{8\rho_\sigma}. \tag{S17}$$

In Eqs. (S12) and (S14), $e_{\alpha\beta}^{\mathrm{UEG}}$ and $e_{\sigma\sigma}^{\mathrm{UEG}}$ are the uniform-electron-gas(5) (UEG) correlation energy density for antiparallel-spin and parallel spin situations. The non-linear parameters $\gamma_{C_{\alpha\beta}}$ in Eq. (S13), $\gamma_{C_{\sigma\sigma}}$in Eq. (S15) and α_X, $\alpha_{C_{\alpha\beta}}$, and $\alpha_{C_{\sigma\sigma}}$ in Eq. (S4) (utilized in Eqs. (S2), (S12) and (S14)) are taken from previous work(2, 3, 6, 7).

The parameters X in Eq. (S1), a_i and d_i in Eq. (S2), $c_{C_{\alpha\beta,i}}$ and $d_{C_{\alpha\beta,i}}$in Eq. (S12), and $c_{C_{\sigma\sigma,i}}$ and $d_{C_{\sigma\sigma,i}}$ in Eq. (S14) were optimized against the data in the training set of Minnesota Database 2017(8, 9). During this process, we enforced the following constraint to satisfy the correct UEG limit for the exchange energy,

$$a_0 + d_0 + X/100 = 1 \tag{S18}$$

The UEG limit was not strictly enforced in the VSXC functional. Previous studies have demonstrated that violations of the UEG limit can improve the accuracy for atomic and molecular energies,(8-11) which is not surprising because real atoms and molecules do not resemble the mathematical model that constitutes the uniform electron gas. In this work, we also observed that the overall errors are reduced when the UEG limit for the correlation part is not strictly satisfied. Therefore, we did not retain the UEG limit for the correlation energy in revM06.

The parameters of the new functional were determined by minimizing

$$F = \sum_{n=1}^{27} R_n/I_n + \lambda S \tag{S19}$$

where R_n is the root mean squared error of subdatabase *n* of the Minnesota Database 2017 (see Section 1.2 for a description of the database) with reference to the experimental data or calculated results using high-level wave function theories,

$$R_n = \sqrt{\frac{\sum_{i=1}^{N}(E_i^{\mathrm{cal}} - E_i^{\mathrm{ref}})^2}{N}} \tag{S20}$$

I_n is the inverse weight of that subdatabase of subdatabase *n* in Table S1, and E_i^{cal} and E_i^{ref} are the calculated data and reference value, respectively, for the *i*th system in subdatabase n. Each term in the first summation of Eq. (S19) corresponds to one of the 27 subdatabases in Table S1. S is a measure of nonsmoothness.

The inverse weights were initially assigned the same values as those used in the revM06-L functional and then adjusted based on the results of preliminary fits. During the optimization we constrained the local exchange functional to go to the correct uniform-electron-gas(5) (UEG) limit, but we did not constrain the local correlation functional. The smoothness restraint is the same as that utilized in the optimization of the revM06-L functional.(1) A key aspect of our procedure is that we manually adjust the inverse weights to try to achieve good performance across all 27 subdatabases.

In the present work, we chose the same value of λ, namely 0.01 as that used in previous work(1, 8, 10). The converged revM06-L orbitals of each system were employed as the initial guess for the first-round of optimization of the revM06 functional. Then all parameters of revM06 were fitted in a self-consistent fashion as described in ref. (1).

Table S3 gives the values of all the linear parameters of the revM06 functional. As shown in Table S3, the largest absolute value among all parameters is about 4.24, which is significantly smaller than those in M06 and M06-2X; this shows that the smoothness restraints successfully reduce the magnitudes of the parameters. The percentage (X) of Hartree-Fock exchange in the revM06 functional is 40.41, which is very close to the average value (40.5) of M06 (27) and M06-2X (54). It is interesting that the percentage of Hartree-Fock exchange in recently developed MN15 functional is 44, which is also close to the optimized value obtained in the present study.

As stated above, the functional form of the local part of revM06 is the same as for revM06-L, in which we removed some large integral terms of the M06-L exchange-correlation energies, including the terms with the coefficients of d_1, d_3, d_4, *and* d_5 in the exchange energy of Eq. (S3), and $d_{C_{\alpha\beta,3}}$, $d_{C_{\alpha\beta,4}}$, and $d_{C_{\sigma\sigma,3}}$, $d_{C_{\sigma\sigma,4}}$ in the correlation energy form of Eqs. (S12) and (S14), respectively. Especially noteworthy is that in the original M06 and M06-2X functionals, $d_{C_{\alpha\beta,5}}$ and $d_{C_{\sigma\sigma,5}}$ in Eqs. (S12) and (S14), respectively, were both set to zero, but in revM06, these two parameters were optimized by fitting against the training set. We found that adding these two terms in the revM06 functional also improved the overall performance on the training set. Therefore, the number of parameters in revM06 is one greater than in revM06-L, namely 32 (31 parameters in the local part plus X). For comparison, the original M06 and M06-2X functionals have 33 and 29 independent parameters, respectively. (The numbers of parameters are mentioned just for completeness; the number of parameters is not a good way to judge the quality of a functional.)

1.2 Databases for training and testing

The aim of designing the revM06 functional is to obtain improved across-the-board accuracy for applications involving both main-group and transition-metal elements. We use two major databases, each of which has a number of subdatabases.

The first major database is Minnesota Database 2017; this database is a modified version of Minnesota Database 2015A which we used previously.(8, 9) A number of changes were made on going from Database 2015A to Database 2017. First we omitted the lattice constant subdatabase (LC17) because the present functional is designed primarily for molecules – not solids (although it can be used for solids if desired). Second, we updated the basis sets used for some elements in subdatabase AE17:

Atom	previous	new
Li	cc-pCVQZ	cc-pwCV5Z
Be	cc-pCVQZ	cc-pwCV5Z
Na	cc-pCV5Z	cc-pwCV5Z
Mg	cc-pCV5Z	cc-pwCV5Z
Al	cc-pwCVQZ	cc-pwCV5Z

Third, four data were removed due to the uncertainty of reference values. Fourth, the reference values were updated for some of the systems based on more accurate values reported in the literature recently and also to correct some errors.

An early version of database 2017 was used for the parameterization. Table S1 gives a brief description of each of the 27 subdatabases, gives references for the data, and gives the inverse weights used in Eq. (S19).

Database 2017 has 418 energetic data (collected as database AME418) and 10 diatomic bond lengths (collected as database MS10).

The second major database is Minnesota Database 2018. This includes all of Database 2017 plus nine more (sub)databases. The additional databases are used only for testing – not for parameterization. The additional databases are given in Table S2. These test sets includes six databases that we have used previously, namely 13 alkyl bond dissociation energies (database ABDE13), 528 interaction energies relevant to biomolecular structures (database S66x8 and its subdatabase S66), excitation energies of 30 valence and 39 Rydberg states of 11 organic molecules (database EE69), 22 transition metal (TM) reaction barrier heights (database TMBH22), 9 ligand dissociation energies of large cationic TM complexes (database WCCR9), and 7 bond lengths of homonuclear TM dimers (database TMDBL7). It also includes nine databases taken from the work of Goerigk and Grimme.(12) These nine databases are 6 dimerization energies of AlX_3 compounds (AL2X6), 10 diverse reaction barrier heights (BHDIV10), 26 barrier heights of pericyclic reactions (BHPERI26), 27 barrier heights for rotation around single bonds (BHROT27), 10 double-ionization potentials of closed-shell systems (DIPCS10), 11 dissociation energies in heavy-element compounds (HEAVYSB11), 13 proton-exchange barriers in H_2O, NH_3, and HF clusters (PX13), 16 self-interaction errors (SIE4x4), and 18 ylide bond-dissociation energy (YBDE18). There are overall 786 data in these non-training test sets, including 779 molecular energies and 7 bond lengths. Therefore, the full set of data agents which revM06 is tested consists of 1197 energetic data and 17 geometric data for a total of 1214 data, plus the Ar_2 and Kr_2 potential energy curves.

The new revM06 functional was optimized against an early version of Database 2017, and tests on re-optimizing it against Database 2017 showed little improvement. Therefore, revM06 was not re-optimized against Database 2017. However, the performance of all functionals used in this study was evaluated based on the final versions of Databases 2017 and 2018.

Based on more accurate values reported in the literature recently, the reference/experimental values were updated for some of the databases or for some of the systems in a database. All reference values are listed in Table S22. The databases with such changes are:

- HTBH38/18 and NHTBH38/18 databases – The reactions are the same as in our previous barrier height databases, but we updated all the data to new reference values taken from the work of Goerigk and Grimme.(12) The use of the new values is indicated by the suffix "/18". The union of these two databases is BH76/18.

- NCCE30/18 and NGD21databases – New reference values for the NCCE30 database were taken from the work of Pernal and coworkers(13). In our recent work(9) we reorganized the NCCE31 database such that four noble gas dimers (HeNe, HeAr, Ne_2, and NeAr) were removed from it and three complexes, CO_2···Ar, parallel-displaced $(CO_2)_2$ (denoted as $(CO_2)_2$PD), and pyridine dimer $(C_5H_5N)_2$, were added to it, resulting in the NCCE30 database. The four noble gas dimers were made part of the NGD21 database. Therefore, the reference values of the 27 complexes in NCCE30 and the four noble gas dimers in NGD21 that were originally part of NCCE30 are from the work of Pernal and coworkers(13). To distinguish the new data from the previous incarnation of NCCE30, we label the updated one NCCE30/18.
- 3dEE8, 4dAEE5, and pAEE5 databases – The new experimental values taken from the NIST website(14) or Moore's tables(15) include spin-orbit coupling (SOC). Therefore, the theoretically calculated values with all the methods also have SOC added to them.
- MR-TM-BE13 database – The reference values of TiCl, NiCl, and CuCl in the MR-TM-BE13 database were updated based on recent reports in literature about more accurate experimental values for these systems(16, 17).
- DC9/18 database – The reference value for one reaction in the DC9 database ($C_6Cl_6 + 6HCl \rightarrow 6Cl_2 + C_6H_6$) was updated from the work of Goerigk and Grimme.(12) The updated database is named DC9/18.

The other changes to Database 2015A include fixing mistakes in some SOC values and removal of some data points for which we now believe the reference values are too uncertain to be used for either parameterization or testing. CoH and FeH were removed from the SR-TM-BE17 database to give the SR-TM-BE15 database. This also causes subset SRMBE12 to be reduced by two. But before that, we note that SRMBE12 should have been given as SRMBE10 (when we fix a typo in the count given in our past work); therefore, after removing two of the compounds (CoH and FeH) it becomes SRMBE8; then we split SRMBE8 into SRMBE4 and SR-TMD-BE4 to show more details on transition-metal dimers. SR-TMD-BE4 and MR-TMD-BE3 were further combined to form TMD-BE7. Furthermore, the subset MBE15 becomes MBE13 and the subset TMBE15 becomes TMBE13 after removal of these two compounds. CuH was removed from the MR-TM-BE13 database resulting in the MR-TM-BE12 database, which was renamed to MR-TML-BE12. LiO was removed from the SR-MGM-BE9 database, which led to SR-MGM-BE8. Also, the subset MGDSR5 becomes MGDSR4.

In the present work, all reference energies include spin-orbit coupling (SOC) since it is automatically present in experiment. All DFT calculations were, however, done without spin-orbit coupling. Therefore, the effect of SOC was added to all DFT energies before comparing to the reference values. Note that, to first order, SOC is zero by symmetry for closed-shell molecules, for linear molecules in Σ states, and for singlet and doublet molecules in A or B states. A polyatomic molecule with no symmetry axis of order 3 or higher must be in an A or a B state; so if it is a singlet or a doublet, we set the SOC equal to zero without further consideration. For cases that remain, the SOC can be nonzero and was treated as follows:

- For atoms and atomic ions, we calculated the SOC from the NIST tables(14) or Moore's tabulations(15) of atomic data.
- For molecules, if the system has no atom heavier than N, we neglected SOC.
- For other molecules, we took the value from the literature, when available.
- In a few cases, SOC need not be zero but it was not available in the literature. In those cases, the SOC(18) values were calculated using *Molpro* version 2010.1.24(19). In particular, state-averaged complete active space self-consistent field (SA-CASSCF)(20-26) calculations were performed with the correlation-consistent polarized valence double-zeta (cc-pVDZ)(27, 28) basis set. The SA-CASSCF/cc-pVDZ calculations were done without including any SOC terms, and this was followed by state-interaction calculations(29-31), to obtain the SOC values. This was done for six systems in the SR-TML-BE11 database ($CrCl_2$, MnF_2, $FeCl_2$, $CoCl_2$, $CrCH_3^+$, VCO^+), for two systems in the MR-MGN-BE17 database (SO (m

= 3) and S_2), for three systems in the MR-TML-BE12 database (CrOF, $(FeBr_2)_2$, $Fe(CO)_5$), for three systems in the IP23 database (Cl_2^+, PH^+, S_2^+) and for five systems in the EA13 database (PH_2, S_2, O_2^- (anion), PH^- (anion), S_2^- (anion)).

The SOC values we added to the DFT calculations are listed in Table S19. The value is not listed when it is taken as zero.

1.3 Computational details

All the calculations were performed using a locally modified version(32) of the *Gaussian 09* program.(33) The molecular geometries and quadrature grids for calculations on Database 2017 (which is the entire training set and part of the test set in this work) are the same as those employed in our previous work on the development of the MN15-L, MN15, and revM06-L functionals.(1, 8, 10) The basis sets are listed in Table S21. The molecular geometries of systems using for parametrization of the earlier GAM functional are given in the supporting information of that paper(9). The geometries of systems added after the parametrization of GAM are given in Table S23.

Table S1. Database 2017 (Refs. 34-53)

This is the subset of Database 2018 that was used for training. In databases and subdatabases named X*n*, there are *n* data; in those named X*n*/*yy*, there are *n* data, and *yy* represents the year in which data was updated. Inverse weights have units of kcal/mol per bond for subdatabases 1-25 and Å for subdatabases 26, 27. TM is short for transition metal.

Subdatabase number	Subdatabase group	Subdatabase	Subsubdatabase	Description	weights	ref	Number of data			
							SR	MR	Other	Total
1-4	MGBE136			main-group bonding energies						
1		SR-MGM-BE8		single-reference main-group metal bond energies	2.00		8			8
			SRM2	single-reference main-group bond energies		(47)				
			SRMGD4	single-reference main-group diatomic bond energies		(47, 48)				
			3dSRBE2	3d single-reference metal−ligand bond energies		(49)				
2		SR-MGN-BE107		single-reference main-group non-metal bond energies	0.11	(47)		107		
3		MR-MGM-BE4		multi-reference main-group metal bond energies	1.00	(48)			4	
4		MR-MGN-BE17		multi-reference main-group non-metal bond energies	1.67	(47)			17	
5-7	TMBE30[f]			transition metal bonding energies						
5		SR-TML-BE11		single-reference TM bond energies	1.35		11			11
			3dSRBE4	3d single-reference metal−ligand bond energies		(49)				
			SRMBE4	single-reference metal bond energies		(47)				
			PdBE2	palladium complex bond energies		(50)				
			FeCl	FeCl bond energy		(51)				

6		MR-TML-BE12		multi-reference TM bond energies	1.01			12		12
			3dMRBE6	3d multi-reference metal−ligand bond energies		(49)				
			MRBE3	multi-reference bond energies		(47)				
			remaining	bond energies of remaining molecules: VO, CuCl, NiCl		(51)				
7		TMD-BE7		TM dimer bond energies						
			SR-TMD-BE4	single-reference TM dimer bond energies (Cu2,CuAg,Zr2,Ag2)	1.35	(47)	4			4
			MR-TMD-BE3	multi-reference TM dimer bond energies (V2,Cr2,Fe2)	5.0	(47, 52)		3		3
8-9	BH76/18			reaction barrier heights						
8		HTBH38/18		hydrogen transfer barrier heights	0.25	(47)	37	1[a]		38
9		NHTBH38/18		non-hydrogen transfer barrier heights	0.20	(47)	35	3[b]		38
10-11	NC51			noncovalent interactions					51	51
10		NCCE30/18		noncovalent complexation energies	0.028	(44-47, 53)				
11		NGD21		noble gas dimer weak interactions	0.010	(43, 47)				
12-14	EE18			excitation energies (mainly atomic)						
12		3dEE8		3d TM atomic excitation energies and first excitation energy of Fe2	1.78	(42, 48, 52)	8			8
13		4dAEE5		4d TM atomic excitation energies	8.97	(41)	5			5
14		pAEE5		p-block atomic excitation energies	7.81	(40)	5			5
15-17	IsoE14			isomerization energies						
15		4pIsoE4		4p isomerization energies	2.00	(39)	4			4
16		2pIsoE4		2p isomerization energies	2.00	(39)	4			4
17		IsoL6/11		isomerization energies of large molecules	1.80	(47)	6			6

18-19	HCTC20		hydrocarbon thermochemistry						
18		πTC13	thermochemistry of π systems	5.75	(47)	13			13
19		HC7/11	hydrocarbon chemistry	3.50	(47)	4	3[c]		7
	Misc73		miscellaneous data						
20		EA13/03	electron affinities	2.96	(47)	13			13
21		PA8	proton affinities	2.23	(47)	8			8
22		IP23	ionization potentials	3.64	(42, 47)	23			23
23		AE17	atomic energies	5.00	(47)			17	17
24		SMAE3	sulfur molecules atomization energies	5.00	(36-38)	1[d]	2		3
25		DC9/18	difficult cases	10.00	(47)	1[e]	8		9
1-25	AME418					297	53	68	418
26		DGL6	diatomic geometries of light-atom molecules	0.010	(47)				
27		DGH4	diatomic geometries of heavy-atom molecules (ZnS, HBr, NaBr, Ag_2)	0.010	(34, 35)				
26-27	MS10								

[a]O + HCl → OH + Cl (for) in MR, others in SR

[b]H + N2O → OH + N2 (rev)， H + F2 → HF + F (rev)， CH3 + FCl → CH3F + Cl (rev) in MR, others in SR

[c]E31-E1, DE (rxn c), and DE (rxn d) in MR, others in SR

[d]H2S2 in SR, others in MR

[e]HCN···BF3 → HCN+BF3 in SR, others in MR

[f]TMBE30 consists of TML-BE23 and TMD-BE7; TML-BE23 is the combination of SR-TML-BE11 and MR-TML-BE12; TMD-BE7 is the combination of SR-TMD-BE4 and MR-TMD-BE3.

Table S2. Databases used only for testing[a]

Number	Database	Description	ref
1	AL2X6	Dimerization energies of AlX_3 compounds (6 data)	(12)
2	BHDIV10	Diverse reaction barrier heights (10 data)	(12)
3	BHPERI26	Barrier heights of pericyclic reactions (26 data)	(12)
4	BHROT27	Barrier heights for rotation around single bonds (27 data)	(12)
5	DIPCS10	Double-ionization potentials of closed-shell systems (10 data)	(12)
6	HEAVYSB11	Dissociation energies in heavy-element compounds (11 data)	(12)
7	PX13	Proton-exchange barriers in H_2O, NH_3, and HF clusters (13 data)	(12)
8	SIE4x4	Self-interaction-error (16 data)	(12)
9	YBDE18	Ylide bond-dissociation energy (18 data)	(12)
10	ABDE13	Alkyl bond dissociation energies (13 data)	(54)
11	S66x8	Interaction energies relevant to biomolecular structures (528 data)	(55)
12	EE69	Excitation energies of 30 valence and 39 Rydberg states of 11 organic molecules (69 data)	(56)
13	TMBH22	TM reaction barrier heights (Mo, W, Zr, Re) (22data)	(57-59)
14	WCCR9	Ligand dissociation energies of large cationic TM complexes (9 data)	(60, 61)
15	TMDBL7	Bond lengths of homonuclear TM dimers (7 data)	(34)

[a]The first nine of these databases are subdatabases of Minnesota Database 2018, and the next six are used for tested selected functionals. Databases 1-14 are energetic databases, and database 15 is a geometric database. Databases 1-9 are taken from the work of Grimme and coworkers, and databases 10-15 are ones we have used previously.

Table S3. Optimized parameters of the revM06 functional

Index i	a_i	d_i	$d_{C_{\alpha\beta},i}$
0	0.6511394014	-0.05523940140	-0.3390666720
1	-0.1214497763		0.003790156384
2	-0.1367041135	-0.003782631233	-0.02762485975
3	0.3987218551		
4	0.6056741356		
5	-2.379738662		0.0004076285162
6	-1.492098351		
7	3.031473420		
8	0.5149637108		
9	2.633751911		
10	0.9886749252		
11	-4.243714128		
X	40.41		
Index i	$d_{C_{\sigma\sigma},i}$	$c_{C_{\alpha\beta},i}$	$c_{C_{\sigma\sigma},i}$
0	-0.1467095900	1.222401598	0.9017224575
1	-0.0001832187007	0.6613907336	0.2079991827
2	0.08484372430	-1.884581043	-1.823747562
3		-2.780360568	-1.384430429
4		-3.068579344	-0.4423253381
5	0.0002280677172		

2. Additional tables of results

Table S4. Mean unsigned errors (kcal/mol) for the AME418, MR53, and SR297 databases and the eight database groups of AME418 [l]

	Database groups								Databases		
Functional	**MGBE136**[a]	**TMBE30**[b]	**BH76**[c]	**NC51**[d]	**EE18**[e]	**IsoE14**[f]	**HCTC20**[g]	**Misc73**	**MR53**[h]	**SR297**[i]	**AME418**[j]
MN15	**1.21**[l]	5.37	1.36	**0.24**	6.94	**1.41**	3.59	**3.36**	**4.84**	**1.75**	**2.16**
revM06	**1.50**	8.03	**1.30**	**0.24**	**5.73**	**1.65**	**2.63**	**2.76**	6.43	**1.81**	**2.24**
MN15-L	**1.56**	**4.85**	1.66	0.49	**3.41**	2.20	4.54	3.76	**4.22**	**1.99**	**2.31**
M06	1.80	6.52	2.30	0.36	7.96	1.66	3.83	3.60	5.80	2.55	2.73
revM06-L	1.97	6.33	2.12	0.39	7.10	3.51	5.78	4.61	**5.34**	3.00	3.03
B97-1	1.96	**4.90**	4.06	0.54	6.55	2.32	6.76	4.05	6.43	2.98	3.18
M06-2X[k]	1.78	20.27	**1.26**	**0.25**	7.27	1.93	**1.72**	**3.05**	13.73	2.01	3.29
ωB97X-D	2.20	8.90	3.18	0.27	7.91	1.75	5.68	3.97	9.28	2.70	3.33
M08-HX[k]	2.74	18.69	**0.94**	0.29	**5.06**	**1.26**	**2.93**	3.75	14.15	2.13	3.50
M06-L	2.47	**4.25**	4.14	0.43	7.35	2.91	5.52	5.28	6.17	3.36	3.51
GAM	2.67	5.07	5.43	0.68	6.56	3.29	7.77	8.06	9.41	3.94	4.47
B3LYP	2.99	6.89	4.52	0.85	6.65	3.67	9.80	8.64	9.87	3.80	4.78
PBE0	2.63	10.40	3.99	0.54	7.58	1.88	7.26	12.09	10.72	3.21	5.24
TPSS	2.75	5.82	8.50	0.91	6.51	3.32	8.94	8.45	9.29	4.55	5.27
τ-HCTH	2.77	6.52	6.53	0.85	14.41	3.53	10.70	8.20	9.46	4.80	5.34
MGGA_MS2	3.69	7.15	6.39	0.63	11.13	2.74	10.38	9.22	10.97	4.98	5.63
VSXC	2.41	6.89	5.07	1.72	8.02	4.27	10.56	15.36	8.40	3.98	6.09
PW6B95-D3(BJ)	1.67	6.07	3.37	0.40	6.01	1.74	4.68	25.67	6.75	2.51	6.66
PBE	4.88	8.63	9.06	0.88	6.49	2.32	5.02	15.98	14.21	4.94	7.35

[a]The MGBE136 subdatabase of main-group bond energies consists of SR-MGM-BE8, SR-MGN-BE107, MR-MGM-BE4, and MR-MGN-BE17.

[b]The TMBE30 subdatabase of transition-metal bond energies consists of SR-TML-BE11, MR-TML-BE12, and TMD-BE7.

[c]The BH76 subdatabase of barrier heights consists of HTBH38/18 and NHTBH38/18.

[d]The NC51 subdatabase of noncovalent interaction energies consists of NGD21 and NCCE30/18.

[e]The EE18 subdatabase of atomic electronic excitation energies consists of 3dEE8, 4dAEE5, and pAEE5.

[f]The IsoE14 subdatabase of isomerization energies of large molecules consists of 2pIsoE4, 4pIsoE4, and IsoL6/11.

[g]The HCTC20 of hydrocarbon energetics consists of HC7/11 and πTC13.

[h]The MR53 are the 53 multi-reference systems defined by generalized B1 diagnostics(62-64). Details are given in ref. (10).

[i]The SR297 are the 297 single-reference systems defined by generalized B1 diagnostics(62-64). Details are given in ref. (10).

[j]The AME418 database consists subdatabases 1–25 in Table S1 of the Supporting Information.

[k]The M06-2X and M08-HX density functionals were designed in previous work for use on main-group chemistry; transition metal chemistry was explicitly excluded as a recommended use when they were published, and the errors of these functionals for transition-metal-chemistry are included here only to remind users of the potentially poor performance if these functionals are used outside their recommended domain.

[l]The results for three best-performing functionals for each subdatabase and for the whole database are highlighted in bold.

Table S5. The MUEs (kcal/mol) for the AME418 database and three specialized subdatabases: one excluding AE17 (AMExAE401), one excluding TMD-BE7 (AMExTMdBE411), and one excluding both AE17 and TMD-BE7 (AMExAExTMdBE394)

Functionals	AME418	AMExAE401	AMExTMDBE411	AMExTMDBExAE394
MN15	**2.16**	**2.00**	**1.96**	**1.79**
revM06	**2.24**	**1.91**	**2.18**	**1.83**
MN15-L	**2.31**	**2.16**	**2.09**	**1.92**
M06	2.73	2.48	2.65	2.39
revM06-L	3.03	2.90	2.97	2.83
B97-1	3.18	3.03	3.09	2.93
M06-2X	3.29	2.36	3.33	2.36
ωB97X-D	3.33	2.89	3.22	2.77
M08-HX	3.50	2.57	3.46	2.49
M06-L	3.51	3.49	3.36	3.33
GAM	4.47	4.43	4.22	4.18
B3LYP	4.78	4.60	4.20	4.00
PBE0	5.24	4.79	3.84	3.34
TPSS	5.27	5.24	4.71	4.68
τ-HCTH	5.34	5.21	4.85	4.70
MGGA_MS2	5.63	5.46	5.18	4.99
VSXC	6.09	5.93	4.22	4.03
PW6B95-D3(BJ)	6.66	6.51	2.76	2.53
PBE	7.35	7.29	5.67	5.57

Table S6. The MUEs (kcal/mol) for the 25 energetic subdatabases of AME418

Name	revM06	M06	M06-2X	revM06-L	M06-L	MN15-L	MN15
SR-MGM-BE8	1.84	4.06	1.58	2.45	3.79	2.61	1.55
SR-MGN-BE107	0.86	1.14	0.84	1.71	1.93	1.39	0.84
MR-MGM-BE4	6.42	5.00	10.45	6.44	11.92	1.88	3.92
MR-MGN-BE17	4.20	4.13	5.75	2.32	2.99	2.08	2.79
SR-TML-BE11	1.89	2.90	4.91	6.14	4.62	2.58	2.61
MR-TML-BE12	5.68	3.58	12.40	3.82	3.53	3.12	4.13
TMD-BE7	21.67	17.27	57.89	10.93	4.91	11.38	11.81
HTBH38/18	1.52	2.35	1.33	2.04	4.56	1.29	1.06
NHTBH38/18	1.09	2.25	1.19	2.19	3.73	2.03	1.66
NCCE30/18	0.38	0.49	0.34	0.61	0.65	0.81	0.39
NGD21	0.04	0.19	0.11	0.07	0.13	0.02	0.02
3dEE8	7.67	9.94	7.56	8.29	7.24	3.89	9.16
4dAEE5	3.89	7.28	9.28	4.97	7.16	1.07	5.86
pEE5	4.46	5.46	4.79	7.34	7.73	4.98	4.49
IsoL6/11	0.97	1.27	1.53	1.32	2.76	1.32	1.80
2pIsoE4	1.91	1.60	1.77	4.41	3.16	1.95	0.27
4pIsoE4	2.40	2.31	2.71	5.88	2.88	3.75	1.96
πTC13	2.76	4.40	1.49	7.02	6.69	4.84	3.52
HC7/11	2.38	2.78	2.15	3.48	3.35	3.98	3.72
IP23	3.07	4.95	3.39	4.49	3.93	2.47	2.50
EA13/03	1.64	1.79	2.12	5.43	3.76	2.12	0.94
PA8	1.57	1.84	1.65	2.62	1.88	2.17	1.14
AE17	3.77	4.49	2.28	4.42	7.15	7.58	6.90
DC9/18	2.53	3.22	4.58	5.55	10.27	3.77	5.32
SMAE3	3.36	1.88	8.08	5.65	5.74	3.33	0.53

Table S7. The MUEs (Å) for the MS10 subdatabase group and its constituent subdatabases

Type	**Subtype**	**Functional**	**MS10**	**DGL6**	**DGH4**
Local	GGA	PBE	0.016	0.013	0.021
	NGA	GAM	0.019	0.007	0.036
	meta-GGA	VSXC	0.012	0.006	0.021
		τ-HCTH	0.011	0.006	0.019
		TPSS	0.012	0.010	0.014
		M06-L	**0.007**	**0.006**	**0.009**
		revM06-L	**0.009**	**0.009**	**0.009**
		MGGA_MS2	0.010	0.007	0.014
	meta-NGA	MN15-L	0.012	0.004	0.024
Nonlocal	Global-hybrid GGA	B3LYP	0.017	0.009	0.028
		PBE0	0.008	0.003	0.014
		B97-1	0.015	0.006	0.027
	RS-hybrid GGA+MM	ωB97X-D	0.012	0.005	0.023
	Global-hybrid meta-GGA	**M06**	**0.012**	**0.006**	**0.022**
		M06-2X	**0.022**	**0.004**	**0.048**
		revM06	**0.012**	**0.008**	**0.018**
		M08-HX	0.022	0.005	0.047
	Global-hybrid meta-GGA + MM	PW6B95-D3(BJ)	0.010	0.007	0.015
	Global-hybrid meta-NGA	MN15	0.007	0.005	0.011

Table S8. Performance on nine databases added to Database 2017 to make Database 2018[a]

Functionals	AL2X6	BHDIV10	BHPERI26	BHROT27	DIPCS10	HEAVYSB11	PX13	SIE4x4	YBDE18	Average[b]
M08-HX	2.18	**1.03**	1.60	0.41	3.34	3.15	2.63	**8.64**	**2.15**	**2.59**
revM06	0.92	1.27	2.25	0.67	**2.73**	**2.15**	**1.11**	11.28	3.04	**2.89**
M06-2X	**0.87**	**1.03**	1.36	**0.36**	3.10	8.34	5.38	**8.63**	**2.48**	**3.18**
MN15	1.46	1.71	**1.25**	0.48	4.33	5.07	2.03	11.30	3.37	3.20
PW6B95-D3(BJ)	**0.59**	2.59	**1.06**	0.56	**2.75**	**1.39**	1.47	15.34	3.25	3.20
ω B97X-D	3.08	**1.22**	2.16	**0.39**	5.42	2.17	1.51	13.37	2.81	3.35
PBE0	2.76	4.25	**1.28**	0.59	**2.94**	3.63	6.19	14.13	**2.54**	3.87
M06	3.04	1.89	2.26	0.69	6.49	**1.85**	**1.47**	14.23	4.90	3.90
B97-1	4.97	3.51	1.73	**0.38**	4.60	3.11	3.72	16.59	4.96	4.40
MN15-L	1.38	2.07	1.79	0.87	10.30	6.45	6.37	**10.99**	4.19	4.43
M06-L	**0.79**	3.07	1.92	0.99	8.42	2.74	**0.90**	17.92	4.90	4.47
MGGA_MS2	1.28	4.87	3.89	0.55	4.59	2.49	2.46	18.48	4.44	4.77
revM06-L	1.48	2.43	3.91	1.12	9.50	2.65	6.01	14.17	5.51	5.06
GAM	7.09	4.63	2.51	0.70	7.78	5.14	1.55	22.94	4.70	5.69
B3LYP	8.88	2.75	4.33	0.41	4.39	7.64	3.63	17.60	8.19	5.90
VSXC	10.48	3.67	2.99	1.66	5.47	5.49	4.18	21.71	4.80	6.02
TPSS	3.98	6.08	2.23	0.54	3.80	4.45	8.38	21.54	7.31	6.05
τ-HCTH	9.82	5.59	2.80	0.46	4.06	6.84	8.95	22.94	7.18	6.78
PBE	4.25	8.22	3.93	0.47	4.59	4.58	11.57	23.42	5.91	6.94

[a]The average MUE of all 137 data in the nine databases.

[b]The three best-performing functionals for each subdatabase and for the whole database are highlighted in bold.

Table S9. The MUEs (kcal/mol) for barrier heights

Functionals	NewBH76[a]	BH76/18[b]	BH152[c]
M08-HX	1.28	0.94	1.11
MN15	1.17	1.36	1.27
revM06	**1.37**	**1.30**	**1.33**
M06-2X	**1.65**	**1.26**	**1.45**
M06	**1.52**	**2.30**	**1.91**
MN15-L	2.28	1.66	1.97
ωB97X-D	1.30	3.18	2.24
PW6B95-D3(BJ)	1.15	3.37	2.26
revM06-L	**3.08**	**2.12**	**2.60**
M06-L	**1.56**	**4.14**	**2.85**
B97-1	1.82	4.06	2.94
PBE0	2.27	3.99	3.13
B3LYP	2.61	4.52	3.56
GAM	1.98	5.43	3.71
VSXC	2.81	5.07	3.94
MGGA_MS2	2.59	6.39	4.49
τ-HCTH	3.38	6.53	4.96
TPSS	3.19	8.50	5.84
PBE	4.57	9.06	6.82

[a]The NewBH76 subdatabase group includes BHDIV10, BHPERI26, BHROT27, and PX13.
[b]The BH76/18 subdatabase group includes HTBH38/18 and NHTBH38/18.
[c]The BH152 subdatabase group consists of BH76/18 and NewBH76.

Table S10. The MUEs (in kcal/mol) for the alkyl bond dissociation energy (ABDE13) database

Functional	Type	ABDE13
M08-HX	hybrid meta-GGA	1.27
revM06	**hybrid meta-GGA**	**1.32**
M06-2X	**hybrid meta-GGA**	**1.38**
ωB97X-D	RS-hybrid GGA+MM	1.50
MN15	hybrid meta-NGA	1.80
PW6B96-D3(BJ)	hybrid meta-GGA+MM	1.82
M06	**hybrid meta-GGA**	**2.29**
revM06-L	**meta-GGA**	**2.42**
B97-1	hybrid GGA	4.00
PBE0	hybrid GGA	4.27
MN15-L	meta-NGA	4.62
PBE	GGA	5.08
M06-L	**meta-GGA**	**5.35**
GAM	meta-GGA	6.28
MGGA_MS2	meta-GGA	6.61
B3LYP	hybrid GGA	8.65
VSXC	meta-GGA	9.00
τ-HCTH	meta-GGA	9.73
TPSS	meta-GGA	10.67

Table S11. The MUEs (kcal/mol) of 19 selected density functionals for the S66 and S66x8 databases and the subdatabases of S66

DFT	DD23[a]	HB23[b]	Mix20[c]	S66[d]	S66x8[d]
Without molecular mechanics dispersion terms					
revM06	**0.24**	**0.29**	**0.26**	**0.26**	**0.26**
MN15	0.57	0.36	0.32	0.42	0.32
M06-2X	**0.35**	**0.24**	**0.25**	**0.28**	**0.34**
M08-HX	0.34	0.24	0.28	0.29	0.41
revM06-L	**0.41**	**0.51**	**0.48**	**0.47**	**0.45**
M06-L	**0.69**	**0.39**	**0.73**	**0.60**	**0.51**
M06	**0.83**	**0.43**	**0.71**	**0.65**	**0.56**
GAM	1.88	0.39	0.94	1.08	0.83
MN15-L	2.43	1.35	1.00	1.62	1.06
MGGA_MS2	2.36	0.80	1.20	1.46	1.08
B97-1	3.19	0.70	1.62	1.85	1.35
PBE0	3.58	0.63	1.79	2.01	1.45
PBE	3.63	0.74	1.94	2.11	1.51
TPSS	4.83	1.38	2.77	3.00	2.11
τ-HCTH	5.44	1.56	3.01	3.35	2.32
B3LYP	5.17	1.47	3.00	3.22	2.37
VSXC	16.05	1.79	7.12	8.37	5.78
With molecular mechanics dispersion terms					
PW6B95-D3(BJ)	0.16	0.23	0.15	0.18	0.21
ωB97X-D	0.47	0.28	0.22	0.32	0.23

[a]DD23 is the dispersion-dominated subdatabase; [b]HB23 is the hydrogen bonding subdatabase; [c]Mix20 is the mixed subdatabase; [d]S66 is a subset of S66x8, which contain interaction energies of 66 non-covalently bound complexes at 8 interacting distances, between 0.9 and 2.0 times of the equilibrium distance, whereas S66 contains only the equilibrium distance. S66 is the union of DD23, HB23, and Mix20.

(The results for the M08-HX, GAM, PBE0, τ-HCTH, VSXC, MGGA_MS2, B97-1, and revM06 functionals are new in the present study.)

Table S12. The MUEs (in eV) of 19 selected methods for the vertical excitation energies of 30 valence and 39 Rydberg transitions and also for all 69 transitions

Name	X^a	Valence	Rydberg	All states
MN15	44	0.29	0.24	0.26
M06-2X	**54**	**0.36**	**0.26**	**0.30**
ωB97X-D	22.2-100	0.32	0.28	0.30
revM06	**40.41**	**0.42**	**0.33**	**0.37**
PW6B95-D3(BJ)	28	0.28	0.54	0.43
B97-1	21	0.25	0.60	0.45
M08-HX	52.23	0.38	0.51	0.46
revM06-L	**0**	**0.50**	**0.51**	**0.51**
PBE0	25	0.22	0.80	0.55
B3LYP	20	0.20	1.03	0.67
MGGA_MS2	0	0.29	1.01	0.69
M06-L	**0**	**0.28**	**1.08**	**0.73**
MN15-L	0	0.53	1.02	0.80
GAM	0	0.38	1.16	0.82
M06	**27**	**0.30**	**1.33**	**0.88**
VSXC	0	0.24	1.54	0.97
τ-HCTH	0	0.32	1.53	1.00
TPSS	0	0.26	1.63	1.03
PBE	0	0.40	1.70	1.13

[a]WFT indicates wave function theory. *X* is the percentage of Hartree–Fock exchange. When a range of *X* is indicated, the first value corresponds to small interelectronic separation, and the second to large interelectronic separation. (The results for GAM, MGGA_MS2, B97-1, PW6B95-D3(BJ), and revM06 are new in the present study.)

Table S13. The MUEs (kcal/mol) of transition-metal reaction barrier height[a] (TMBH22) database

Metal[a]	**MUE (Mo)**	**MUE (W)**	**MUE (Zr)**	**MUE (Re)**	**MUE (22)[b]**
M06	**1.12**	**1.19**	**0.75**	**1.87**	**1.25**
PW6B95-D3(BJ)	1.11	1.76	0.90	1.81	1.44
MN15	2.02	2.82	1.51	0.85	1.92
MN15-L	1.30	2.63	0.73	2.67	1.93
revM06	**2.77**	**2.57**	**0.85**	**1.12**	**1.98**
B97-1	1.69	1.96	4.39	1.18	2.15
ωB97X-D	3.72	2.58	1.43	0.79	2.28
PBE0	2.68	2.66	2.66	1.07	2.29
revM06-L	**1.85**	**3.52**	**3.55**	**0.80**	**2.45**
M06-2X	**3.56**	**2.68**	**0.23**	**2.75**	**2.48**
M06-L	**2.57**	**2.32**	**1.22**	**4.12**	**2.61**
MGGA_MS2	3.75	3.85	0.69	1.66	2.75
TPSS	3.70	2.60	3.12	1.56	2.77
B3LYP	1.69	2.31	7.58	1.42	2.92
M08-HX	4.02	3.27	1.45	3.30	3.15
PBE	3.79	3.74	2.63	2.98	3.36
τ-HCTH	3.41	1.72	7.21	2.67	3.40
GAM	2.87	2.55	4.72	4.15	3.40
VSXC	7.12	4.40	13.62	7.96	7.63

[a]There are respectively 6, 7, 4, and 5 reactions in the database for Mo, W, Zr and Re reaction barrier heights. The results of M08-HX, τ-HCTH, VSXC, MGGA_MS2, PW6B95-D3(BJ), B97-1, and revM06 are calculated in the present paper. The revM06-L and ωB97X-D results are from ref. (1). The MN15, MN15-L, and GAM results are from ref. (10). The results for Mo and W of MN15, MN15-L, GAM, revM06-L, and ωB97X-D are recalculated in the present study as the number of reactions changed. All other results are from refs. (57-59).

[b]The mean unsigned error for all 22 barrier heights.

Table S14. The MUEs (kcal/mol) for ligand dissociation energies of large cationic transition-metal complexes (WCCR9)

Functional[a]	Type	WCCR9
M08-HX	hybrid meta-GGA	4.23
revM06	**hybrid meta-GGA**	**4.37**
M06	**hybrid meta-GGA**	**4.49**
MN15-L	meta-NGA	4.76
M06-2X	**hybrid meta-GGA**	**5.19**
M06-L	**meta-GGA**	**5.23**
revM06-L	**meta-GGA**	**5.24**
GAM	NGA	5.26
PW6B95-D3(BJ)	hybrid meta-GGA + MM[b]	5.32
B97-1	hybrid GGA	6.04
MN15	hybrid meta-NGA	6.07
PBE0	hybrid GGA	6.15
MGGA_MS2	meta-GGA	6.89
PBE	GGA	7.12
ωB97X-D	RS-hybrid GGA + MM[b]	7.18
TPSS	GGA	7.37
B3LYP	hybrid GGA	7.5
τ-HCTH	GGA	8.21

[a]VSXC was excluded due to SCF convergence problems for a few systems.
[b]MM denotes empirical dispersion correction.

Table S15. The MUEs (Å) of equilibrium bond lengths for homonuclear transition metal dimers (TMDBL7)

	Cu_2	Au_2	Ni_2	Pd_2	Pt_2	Ir_2	Os_2	MUE(1)[a]	MUE(2)[a]
MGGA_MS2	2.210	2.527	2.080	2.493	2.359	2.254	2.275	0.028	0.028
MN15-L	2.249	2.539	2.116	2.484	2.356	2.244	2.269	0.028	0.035
τ-HCTH	2.262	2.540	2.123	2.489	2.357	2.255	2.274	0.028	0.032
TPSS	2.234	2.538	2.108	2.516	2.365	2.262	2.282	0.029	0.029
PBE	2.242	2.552	2.118	2.507	2.372	2.265	2.283	0.031	0.032
M06-L	**2.214**	**2.555**	**2.101**	**2.500**	**2.380**	**2.274**	**2.294**	**0.033**	**0.034**
revM06-L	**2.178**	**2.541**	**2.060**	**2.494**	**2.359**	**2.249**	**2.271**	**0.039**	**0.037**
MN15	2.293	2.530	2.087	2.485	2.344	2.233	2.253	0.040	0.049
VSXC	2.227	2.572	2.100	2.530	2.383	2.274	2.297	0.041	0.037
PBE0	2.265	2.544	2.079	2.510	2.351	2.244	2.263	0.041	0.044
PW6B95-D3(BJ)	2.271	2.551	2.094	2.520	2.357	2.249	2.268	0.041	0.045
revM06	**2.261**	**2.550**	**2.059**	**2.508**	**2.347**	**2.238**	**2.258**	**0.044**	**0.051**
B3LYP	2.260	2.574	2.086	2.535	2.376	2.265	2.284	0.045	0.047
M06	**2.227**	**2.592**	**2.075**	**2.517**	**2.396**	**2.280**	**2.295**	**0.048**	**0.048**
GAM	2.306	2.609	2.189	2.536	2.408	2.283	2.292	0.059	0.058
M06-2X	**2.367**	**2.588**	**2.101**	**2.540**	**2.351**	**2.232**	**2.250**	**0.066**	**0.073**
M08-HX	2.353	2.599	2.092	2.559	2.358	2.239	2.257	0.069	0.073
B97-1	2.278	2.566	2.391	2.617	2.368	2.259	2.279	0.082	0.073
ωB97X-D	2.259	2.556	2.281	2.694	2.363	2.269	2.369	0.083	0.095
Exp.	2.219	2.472	2.155	2.480	2.333	2.270	2.280	0.000	0.000

[a]The bond lengths in the table and MUE(1) are calculated with the LANL2DZ basis set for comparison with previous work, and MUE(2) is averaged over this basis set and also over the higher-quality def2-TZVP basis set.

3. Rankings

Table S16. The rankings (out of 94 functionals) of 19 selected functionals for the 25 subdatabases of AME418

Functionals	MN15	revM06	MN15-L	PW6B95-D3(BJ)	M08-HX	M06	B97-1	M06-2X	ωB97X-D	revM06-L	PBE0	M06-L	GAM	TPSS	PBE	B3LYP	VSXC	τ-HCTH	MGGA_MS2
SR-MGM-BE8	1	3	21	8	14	56	11	2	20	17	49	52	6	28	18	64	19	50	84
SR-MGN-BE107	1	3	18	10	36	9	23	2	12	28	32	33	50	53	80	55	37	42	67
SR-TML-BE11	7	3	6	2	22	15	16	60	1	79	17	54	55	51	70	39	40	74	42
MR-MGM-BE4	2	13	1	25	34	3	9	66	58	15	50	77	32	18	56	33	31	72	41
MR-MGN-BE17	3	16	1	6	57	15	5	46	54	2	40	4	17	18	85	38	11	25	67
MR-TML-BE12	14	43	3	16	73	9	2	82	12	10	29	8	18	52	74	24	34	6	35
IsoL6/11	36	2	14	28	1	12	39	23	6	13	17	72	48	85	49	67	92	75	64
IP23	5	13	3	14	37	60	4	20	8	48	17	35	47	43	71	63	29	44	73
EA13/03	1	6	24	7	3	9	16	23	10	86	49	75	84	33	30	36	52	27	65
PA8	11	35	61	16	9	45	34	39	67	72	15	49	83	73	21	3	56	80	88
πTC13	9	6	21	39	3	17	58	1	50	57	47	54	80	74	29	42	79	82	90
HTBH38/18	3	18	8	35	1	26	48	10	28	23	45	43	57	81	88	42	51	74	54
NHTBH38/18	14	1	17	34	6	25	36	3	43	24	37	44	54	86	81	49	53	62	73
NCCE30/18	7	6	29	19	10	14	33	3	5	20	30	22	49	65	66	55	87	61	43
AE17	24	3	27	88	6	8	16	1	18	7	82	25	41	67	83	68	84	65	60
HC7/11	12	5	15	4	23	8	31	1	22	10	50	9	30	55	14	78	70	69	46
3dEE8	26	10	1	25	5	33	24	9	17	15	37	7	31	30	22	28	57	91	79
4dAEE5	44	5	1	28	45	67	60	78	63	11	19	65	6	40	21	53	3	90	84
pAEE5	43	42	52	3	1	57	8	48	80	71	59	75	19	6	32	12	60	85	68
DC9/18	15	1	7	26	16	4	43	12	24	18	36	42	90	63	69	53	48	70	64
2pIsoE4	1	19	22	18	9	13	46	17	21	78	31	48	86	66	42	84	79	77	38
4pIsoE4	15	28	75	8	17	26	35	45	33	94	27	56	71	41	32	84	69	73	67
NGD21	2	5	3	17	19	58	11	28	45	7	30	33	1	51	25	74	63	42	18
TMD-BE7	24	57	22	43	89	47	27	88	63	17	71	2	8	6	19	42	39	32	44
SMAE3	1	7	6	45	58	2	18	39	27	22	42	23	29	51	74	68	50	28	64
Average	**13**	**14**	**18**	**23**	**24**	**26**	**26**	**30**	**31**	**34**	**38**	**40**	**44**	**49**	**50**	**50**	**52**	**60**	**61**
Lowest	**44**	**57**	**75**	**88**	**89**	**67**	**60**	**88**	**80**	**94**	**82**	**77**	**90**	**86**	**88**	**84**	**92**	**91**	**90**

Table S17. The rankings (out of 94 functionals) of 19 selected functionals for the AME418 database and some of its grouped subdatabases

Functionals	MGBE136	TMBE30	BH76/18	NC51	EE18	IsoE14	HCTC20	Misc73	MR53	SR297	AME418
MN15	1	8	10	3	24	3	9	3	2	1	1
revM06	**2**	**41**	**7**	**4**	**6**	**10**	**3**	**1**	**6**	**2**	**2**
MN15-L	3	3	16	25	1	34	13	6	1	3	3
M06	**7**	**21**	**26**	**13**	**45**	**11**	**10**	**4**	**4**	**11**	**4**
revM06-L	**12**	**18**	**23**	**18**	**25**	**77**	**26**	**15**	**3**	**22**	**5**
B97-1	11	4	42	29	19	42	33	9	7	20	6
M06-2X	**5**	**86**	**4**	**5**	**29**	**23**	**1**	**2**	**66**	**4**	**7**
ωB97X-D	19	50	33	7	44	16	25	8	21	14	9
M08-HX	40	82	1	11	3	2	7	5	69	5	16
M06-L	**26**	**1**	**44**	**21**	**30**	**60**	**22**	**27**	**5**	**28**	**17**
GAM	37	7	55	43	21	72	51	55	26	44	35
B3LYP	46	27	45	52	22	82	67	62	33	40	43
PBE0	32	60	39	30	35	22	41	77	47	24	52
TPSS	41	13	83	65	17	74	58	59	22	53	54
τ-HCTH	42	20	67	56	90	79	79	57	28	62	58
MGGA_MS2	66	32	65	40	82	56	73	66	49	68	65
VSXC	24	26	52	87	47	88	76	81	18	46	75
PW6B95-D3(BJ)	4	15	34	19	10	14	15	87	12	10	77
PBE	82	47	87	61	16	41	17	82	70	67	82

Table S18. The rankings (out of 94 functionals) of 19 selected functionals for the nine testing subdatabases of Database 2018 taken from the work of Goerigk and Grimme

Functionals	AL2X6	BHDIV10	BHPERI26	BHROT27	DIPCS10	HEAVYSB11	PX13	SIE4x4	YBDE18	MUE(137)[b]	AMUE[c]
M08-HX	22	3	11	24	11	20	30	6	5	1	15
revM06	**8**	**6**	**24**	**73**	**1**	**5**	**7**	**22**	**14**	**6**	**18**
M06-2X	**6**	**2**	**6**	**5**	**9**	**79**	**53**	**5**	**9**	**9**	**19**
PW6B95-D3(BJ)	1	29	1	55	2	1	14	39	17	10	18
MN15	13	17	3	41	33	49	21	23	19	11	24
ωB97X-D	34	5	20	11	62	6	16	26	11	14	21
PBE0	29	53	4	61	5	28	62	29	10	23	31
M06	**33**	**21**	**25**	**75**	**72**	**2**	**13**	**32**	**37**	**26**	**34**
B97-1	48	42	14	6	41	16	37	45	40	32	32
MN15-L	12	24	15	84	88	63	63	21	29	33	44
M06-L	4	37	18	86	84	10	4	53	38	34	37
MGGA_MS2	10	63	63	54	40	7	29	56	32	42	39
revM06-L	14	28	64	90	87	8	60	31	47	48	48
GAM	65	60	35	78	78	52	17	71	34	55	54
B3LYP	77	34	71	21	35	75	36	51	75	56	53
VSXC	83	44	49	93	63	56	44	65	35	58	59
TPSS	42	76	22	52	20	39	78	64	70	59	51
τ-HCTH	82	73	45	37	24	67	81	70	67	68	61
PBE	44	88	65	38	39	41	87	75	53	74	59

[a]The results for revM06, M06-2X, and M06 are in bold to guide the eye with regard to this key comparison.

[b]The ranking of the MUE over the 137 data in these nine databases.

[c]The average of the rankings over the nine databases in this table.

4. Additional tables

Table S19. Spin-orbit coupling (SOC) in kcal/mol[a]

Species	SOC	Species	SOC	Species	SOC
Al	-0.21	FeC^+	-0.28	Ru^+ (quartet)	-4.04
Al ($3s^13p^2$) (quartet)	-0.22	$FeCl_2$	-1.28	Ru^+ (sextet)	-3.02
Al ($3s^23p^1$) (doublet)	-0.21	FeCl	-1.10	S	-0.56
Al	-0.21	FeH	-1.10	S^-	-0.55
Ar ($3s^23p^54s^1$) (triplet)	-0.65	LiO	-0.16	S_2	-0.01
B	-0.03	Mo^+ (quartet)	-0.50	S_2^-	-0.50
Br	-3.51	NaO	-1.22	S_2^+	-0.61
C	-0.09	NH	-0.05	Sc	-0.29
C^+	-0.12	Ni	-2.78	Sc (doublet)	-0.29
C^+ ($2s^12p^2$) (quartet)	-0.09	Ni^+	-1.72	Sc (quartet)	-0.26
C^+ ($2s^22p^1$) (doublet)	-0.12	Ni^+ (doublet)	-1.72	Sc^+	-0.30
Ca^+_1st excited state	-0.10	Ni^+ (quartet)	-2.75	Se	-2.70
CH ($^2\Pi$)	-0.04	NiCl	-1.50	SH	-0.54
CH_3O	-0.19	NO	-0.18	SH^+	-0.54
Cl	-0.84	O	-0.22	Si	-0.43
Cl^+	-0.98	O^-	-0.16	Si^+	-0.55
Cl_2^+	-0.92	O_2^-	-0.20	Si^+ ($3s^1sp^2$) (quartet)	-0.51
ClO	-0.46	O_2^+	-0.28	Si^+ ($3s^23p^1$) (doublet)	-0.55
Co	-2.27	OCH_3	-0.03	Si_2 (triplet)	-0.20
Co^+	-1.99	OH	-0.20	SO (m=3)	-0.003
$CoCl_2$	-2.41	P^-	-0.28	Ti	-0.64
CoH	-2.10	P^+	-0.91	TiCl	-0.50
$CrCH_3^+$	-0.18	Pd (triplet)	-6.10	V	-0.91
$CrCl_2$	-0.71	Pd^+	-4.05	V (quartet)	-0.91
CrOF	-0.08	PH	-0.17	V (sextet)	-0.53
F	-0.38	PH^-	-0.27	V^+	-0.59
F ($2s^22p^43s^1$) (quartet)	-0.47	PH^+	-0.37	VCO^+	-0.46
F ($2s^22p^5$) (doublet)	-0.39	PH_2	-0.002	Y^+ (triplet)	-1.01
$(FeBr_2)_2$	-1.75	Rh	-4.26	Zn (triplet)	-1.10
Fe	-1.15	Rh^+	-4.73	Zr	-2.06
Fe (triplet)	-1.23	Rh^+ (triplet)	-4.73	Zr_2	-3.30
Fe (quintuplet)	-1.15	Ru	-3.94		
FeC	-0.90	Ru^+	-4.04		

[a]All atomic SOC values are computed from Moore's A*tomic Energy Levels* or from the NIST website. Most of the molecular SOC values were obtained from our previous work(9, 65-67) or calculated in this work. In addition, the SOC for NaO is from Ref. (68), the SOC for OCH_3 is from Ref. (69), and the SOC for PH is from Ref. (70).

Table S20. Exchange–correlation functionals tested in this study(1-4, 7-10, 62, 71-137)

Category	Type	Abbrev.	X^a	Year	Method	Ref.
local	LSDA	LSDA	0	1980	GKSVWN5[b]	(72-75)
			0	1980	GKSVWN3[b]	(72-75)
	GGA – SO[c]	GGA	0	2008	SOGGA	(76)
			0	2008	PBEsol	(77)
			0	2011	SOGGA11	(78)
	GGA – other	GGA	0	1986	B86P86	(79, 80)
			0	1987	B86LYP	(79, 81)
			0	1988	BP86	(80, 137)
			0	1988	BLYP	(81, 137)
			0	1989	BR89LYP	(71, 81)
			0	1991	B86PW91	(79, 82)
			0	1991	PW91*c*	(82)
			0	1991	BPW91	(82, 137)
			0	1996	PBE	(4)
			0	1997	mPWPW	(83)
			0	1997	revPBE	(84)
			0	1999	RPBE	(85)
			0	2001	HCTH407	(86)
			0	2001	OLYP	(81, 87)
			0	2001	OPBE	(4, 87, 88)
			0	2005	MPWLYP1W	(89)
			0	2005	PBE1W	(89)
			0	2005	PBELYP1W	(89)
			0	2005	MOHLYP	(62)
			0	2006	B97-D	(90)
			0	2009	MOHLYP2	(91)
			0	2009	OreLYP	(81, 87, 92)
	NGA	NGA	0	2012	N12	(93)
			0	2015	GAM	(9)
	meta-GGA	mGGA	0	1998	VSXC	(2)
			0	2002	τ-HCTH	(94)
			0	2003	TPSS	(95)
			0	2005	TPSSLYP1W	(89)
			0	2006	M06-L	(96)
			0	2009	revTPSS	(97)
			0	2011	M11-L	(98)
			0	2013	MGGA_MS0	(99)
			0	2013	MGGA_MS1	(99)
			0	2013	MGGA_MS2	(99)
			0	2017	revM06-L	(1)
	meta-NGA	mNGA	0	2012	MN12-L	(100)
			0	2015	MN15-L	(8)

nonlocal	global-hybrid GGA	GGAh	100	1987	HFLYP	(81, 101)
			100	1991	HFPW91	(82, 101)
			20	1992	B3PW91	(102, 137)
			20	1994	B3LYP	(81, 103, 137)
			25	1996	PBE0	(104)
			28	1996	B1B95	(105)
			25	1997	mPW1PW	(83)
			25	1997	B1LYP	(106)
			21.98	1998	B98	(107)
			21	1998	B97-1	(108)
			42.80	2000	MPW1K	(109)
			11.61	2001	O3LYP	(88)
			21	2001	B97-2	(110)
			15	2001	B3LYP*	(111)
			21.8	2004	X3LYP	(112)
			21.8	2004	MPW3LYP	(113)
			5	2005	MPWLYP1M	(62)
			26.93	2005	B97-3	(114)
			35.42	2011	SOGGA11-X	(115)
	RS-hybrid GGA[d]	GGArsh	19-65	2004	CAM-B3LYP	(116)
			0-100	2006	LC-ωPBE	(133-136)
			25-0	2006	HSE06	(117, 118)
			0-60-0	2008	HISS	(119)
			0-100	2008	ωB97	(120)
			15.77-100	2008	ωB97X	(120)
	RS-hybrid NGA	NGArsh	25-0	2012	N12-SX	(121)
	RS-hybrid GGA + MM[e]	NGArsh-D	22.2-100	2008	ωB97X-D	(122)
	global-hybrid meta-GGA	mGGAh	10	2002	TPSSh	(123)
			15	2002	τ-HCTHhyb	(94)
			42	2004	BB1K	(105, 124, 137)
			44	2004	MPWB1K	(113)
			31	2004	MPW1B95	(113)
			42	2004	BMK	(125)
			13	2005	TPSS1KCIS	(126)
			41	2005	MPWKCIS1K	(91)
			15	2005	MPW1KCIS	(91)
			22	2005	PBE1KCIS	(127)
			46	2005	PWB6K	(128)
			28	2005	PW6B95	(128)
			28	2005	M05	(3)
			56	2005	M05-2X	(7)
			100	2006	M06-HF	(129)
			27	2008	M06	(130)
			54	2008	M06-2X	(130)

		52.23	2008	M08-HX	(131)
		56.79	2008	M08-SO	(131)
		9	2013	MGGA_MS2H	(99)
		40.41	2018	revM06	present
global-hybrid meta-GGA+MM[e]	mGGAh-D	28	2005	PW6B95-D3(BJ)	(128)
RS-hybrid meta-GGA[d]	mGGArsh	42.8-100	2011	M11	(132)
RS-hybrid meta-NGA	mNGArsh	25-0	2012	MN12-SX	(121)
global-hybrid meta-NGA	mNGAh	44	2015	MN15	(10)

[a] *X* is the percentage of nonlocal Hartree–Fock exchange. When a range is given, the first value is for small interelectronic distances, and the second value is for large interelectronic distances. Details of the functional forms that join these regions of interelectronic separation are given in the references.

[b] GVWN5 denotes the Gáspár approximation for exchange and the VWN5 fit to the correlation energy; GVWN3 denotes Gáspár approximation for exchange and the VWN fit to the correlation energy; these are examples of the local spin density approximation (LSDA), and they have the keyword SVWN5 and SVWN in the *Gaussian 09* program. Note that Kohn-Sham exchange is the same as Gáspár exchange, but Slater exchange (not tested here) is greater by a factor of 1.5.

[c] SO denotes a GGA that satisfies the gradient expansion to second order. PW91 formally satisfies the gradient expansion for exchange to second order but only at such small values of the gradient that for practical purposes it should be grouped with functionals that do not satisfy the gradient expansion to second order.

[d] RS denotes range-separated.

[e] MM denotes molecular mechanics, which in this case corresponds to atom-atom pairwise damped dispersion terms added post-SCF to the calculated energy.

Table S21. The basis sets used for testing density functionals

Primary subset	Secondary	Basis set
SR-MGM-BE8		
	SRM2	def2-QZVP
	SRMGD4	AlCl: def2-QZVP; KOH: Feller's CVQZ (K), jun-cc-pV(Q+d)Z (O), aug-cc-pVQZ (H); NaO: cc-pCVQZ (Na), jun-cc-pV(Q+d)Z (O); LiCl: cc-pCVQZ (Li), jun-cc-pV(Q+d)Z (Cl)
	3dSRBE2	def2-QZVP
SR-MGN-BE107		MG3S
SR-TM-BE15		
	3dSRBE4	def2-TZVP (metal); ma-TZVP (non-metal)
	SRMBE4	def2-TZVP
	PdBE2	SDD-2fg (Pd); cc-pVTZ (non-metal)
	FeCl	aug-pwCVTZ (Fe); aug-pVTZ (Cl)
MR-MGM-BE4		cc-pCVQZ (metal); aug-cc-pCVQZ (non-metal)
MR-MGN-BE17		MG3S
MR-TM-BE12		
	CuCl, NiCl, VO	aug-cc-pwCVTZ (metal); aug-cc-pVTZ (non-metal)
	3dMRBE6	def2-TZVP (metal); ma-TZVP (non-metal)
	MRBE3	def2-TZVP
TMD-BE7		def2-TZVP
IP23		MG3S
NCCE30/18		MG3S
NGD21		aug-cc-pVQZ
3dEE8		cc-pCVQZ (Ca); cc-pVQZ-DK
4dAEE5		cc-pVTZ-DK
pAEE5		cc-pVQZ-DK; aug-cc-pVQZ-DK (F, Ar)
4pIsoE4		cc-pVQZ
2pIsoE4		cc-pVQZ
IsoL6/11		MG3SXP
EA13/03		MG3S
PA8		MG3S
πTC13		MG3S
HTBH38/18		MG3S
NHTBH38/18		MG3S
AE17		cc-pV5Z (H,He); cc-pwCV5Z
HC7/11		6-311+G(2df,2p)
DC9/18		MG3S
SMAE3		MG3S
AL2X6		def2-QZVP
BHDIV10		def2-QZVP
BHPERI		def2-QZVP

BHROT27		def2-QZVP
DIPCS10		def2-QZVP
HEAVYSB11		def2-QZVP
PX13		def2-QZVP
SIE4x4		def2-QZVP
YBDE18		def2-QZVP
ABDE13		def2-TZVP(metal); ma-TZVP(non-metal)
S66x8		def2-QZVP
EE69		6-311(2+,2+)G**
TMBH22		cc-pVQZ(B, C, H, O, N, Br), cc-pV(Q+d)Z(S, P, Cl), cc-pVQZ-PP(W, Mo, Re, Zr)
WCCR9		def2-QZVPP
TMDBL7		def2-TZVP/LanL2DZ
MS10		
DGL6		6-311+G(2df,2p)
DGH4		
	HBr	aug-cc-pVQZ (H), jun-cc-pVQZ (Br)
	NaBr	cc-pCVQZ (Na), jun-cc-pVQZ (Br)
	ZnS	B2 (Zn), aug-cc-pVQZ (S)
	Ag_2	jun-cc-pVTZ-PP

Note: For H through Si, MG3S is the same as 6-311+G(3d2f,2df,2p); for heavier atoms, MG3S is defined in *Lynch, B. J.; Zhao, Y.; Truhlar, D. G. J. Phys. Chem. A 2003, 107, 1384*. Full details of MG3S are available at *https://comp.chem.umn.edu/basissets/basis.cgi*.

Table S22. The reference energetic data (in kcal/mol) of AME418(78, 96, 138)

Systems	reference	revM06	B3LYP	PBE
SR-MGM-BE8				
AlCl3	309.91	313.01	291.90	303.85
AlF3	429.6	432.12	415.79	425.85
KOH	85	87.62	79.99	84.30
NaO	65.23	67.03	64.80	68.51
LiCl	113.9	115.35	109.03	109.45
AlCl	121.56	124.61	116.20	119.77
ZnSe	25.2	24.00	22.58	30.48
ZnCl	53.48	50.78	46.90	52.53
SR-MGN-BE107				
C2H6	97.39	98.63	91.67	96.87
iPr-CH3	95	94.51	84.97	89.61
C2H6O	89.79	90.73	82.08	86.76
iPr-OCH3	91.51	90.69	79.68	83.7
Et-H	108.92	108.49	106.37	104.87
Et-CH3	95.89	96.29	88.24	93.08
Et-OCH3	95.26	91.66	82.14	86.35
Et-OH	100.29	101.38	93.26	99.57
tBu-H	103.86	103.01	99.58	97.32
tBu-CH3	93.67	93.12	81.63	86.16
tBu-OCH3	89.27	89.27	76.16	80.09
tBu-OH	115.02	101.84	91.12	96.99
CH(2∏)	84.18	81.96	85.29	84.51
CH2(3B1)	190.66	190.87	192.02	194.44
CH2(1A1)	181.37	179.69	180.52	178.62
CH3(2A"2)	307.79	306.25	309.84	309.94
CH4	420.34	419.12	420.89	420.1
NH	83.1	80.7	87.87	88.31
NH2	182.59	178.39	187.58	188.24
NH3	298.02	294.66	300.73	301.71
OH	107.19	106.3	107.91	109.55
H2O	232.75	232.06	230.28	233.52
HF	141.25	141.81	138.53	141.21
SiH2(1A1)	151.79	155.31	153.26	147.42
SiH2(3B1)	131.05	132.35	132.68	131.24
SiH3	227.58	228.14	228.1	221.98
SiH4	324.52	325.14	323.3	312.98
PH2	153.2	156.45	158.56	154.44
PH3	242.27	244.42	244.71	239.12
H2S	183.35	183.67	181.48	181.46
HCl	106.66	106.57	104.08	105.43

C2H2	405.35	405.26	402.96	414.68
CH2CH2	563.51	562.81	563.03	571.44
CH3CH3	712.8	711.18	711.36	716.76
HCN	313.34	310.46	313.08	326.04
HCO	279.11	279.86	279.94	294.7
H2CO	374.35	374.73	373.2	385.59
CH3OH	513.22	513.23	511.11	519.53
NH2NH2	438.6	433.32	443.62	452.61
HOOH	268.57	267.05	266.12	281.01
Si2 (mult=3)	75.72	78.42	70.5	79.25
P2	117.59	121.77	115.85	121.47
S2	103.13	107.45	101.77	113.56
Cl2	58.07	59.98	53.11	63.19
SC	171.11	171.06	165.52	178.79
ClF	61.57	62.43	58.24	69.61
Si2H6	535.03	535.65	529.73	519.15
CH3Cl	395.51	395.28	391.58	398.9
CH3SH	473.84	475.03	471.06	477.54
HOCl	165.17	165.18	161.02	173.27
BCl3	322.9	330.64	310.87	332.71
BF3	469.79	482.57	463.36	479.89
C2Cl4	466.28	475.86	448.09	496.5
C2F4	589.36	604.13	582.15	628.83
C3H4 (propyne)	704.79	706.21	702.36	720.82
C4H4O	993.74	1000.69	987.19	1030.93
C4H4S	962.73	968.98	952.88	995.57
C4H5N	1071.57	1076.2	1068.62	1110.71
C4H6 (trans-1,3-butadiene)	1012.37	1012.57	1009.28	1034.35
C4H6 (2-butyne)	1004.13	1005.93	1000.43	1025.6
C5H5N	1237.69	1241.97	1234.97	1284.97
CCH	265.13	263.95	262.47	276.77
CCl4	312.74	317.11	291.84	329.07
CF3CN	639.85	647.77	632.31	679.13
CF4	476.32	489.46	465.98	500.35
CH2OH	409.76	410.64	410.41	421.12
CH3CN	615.84	614.88	615.98	635.43
CH3NH2	582.22	579.14	584	590.75
CH3NO2	601.27	601.05	602	641.46
CHCl3	343.18	346.23	329.18	355.85
CHF3	457.5	466.88	451.48	476.75
ClF3	125.33	128.48	122.7	159.31
H2	109.49	110.39	110.25	104.71
CH2CH	445.91	445.38	447.07	457.74
HCOOCH3	785.26	790.68	781.85	810.81

HCOOH	500.98	505.41	498.03	521.63
PF3	363.87	372.24	354.19	370.39
SH	86.98	88.2	88.14	87.92
SiCl4	384.94	390.67	358.81	381.23
SiF4	574.35	582.05	553.53	567.6
C2H5	603.75	602.65	604.98	611.88
C4H6 (bicylobutane)	987.2	991.83	977.76	1011.27
C4H6 (cyclobutene)	1001.61	1001.66	993.82	1023.83
HCOCOH	633.35	636.41	630.29	662.71
CH3CHO	677.03	678.4	675.12	694.27
C2H4O	650.7	654.14	647.13	669.49
C2H5O	698.64	698.27	694.79	710.32
CH3OCH3	798.05	799.14	795.55	809.67
CH3CH2OH	810.36	810.45	806.19	820.99
C3H4 (allene)	703.2	706.55	704.23	723.86
C3H4 (cyclopropene)	682.74	685.07	678.31	701.38
CH3COOH	803.04	807.6	797.82	827.56
CH3COCH3	977.96	980.21	974.26	999.98
C3H6 (cyclopropane)	853.41	856.06	849.11	867.94
CH3CHCH2	860.61	860.19	858.35	873.53
C3H8	1006.87	1005.3	1003.05	1014.92
C2H5OCH3	1095.12	1096.34	1090.57	1111.06
C4H10 (isobutane)	1303.04	1300.9	1295.23	1313.84
C4H10 (antiperiplanar butane)	1301.32	1299.43	1294.69	1313.05
C4H8 (cyclobutane)	1149.01	1149.31	1141.17	1167.07
C4H8 (isobutene)	1158.61	1158.05	1153.32	1175.33
C5H8 (spiropentane)	1284.28	1291.47	1275.88	1315.19
C6H6	1367.56	1372.7	1360.79	1409.19
CH3CO	581.58	583.46	582.02	603.41
(CH3)2CH	900.75	900	900.44	914.25
(CH3)3C	1199.34	1197.79	1195.62	1216.44
H2CCO	532.32	538.94	533.5	557.87
SR-TML-BE11				
CrCl2	181.13	182.05	169.5	176.48
MnF2	232.26	234.75	233.57	254.45
FeCl2	190.29	193.48	184.93	197.41
CoCl2	182.9	191.87	170.36	186.4
AgH	54	55.21	54.45	55.86
CrCH3+	28.8	33.66	35.01	43.92
CuH2O+	38.8	39.36	38.81	43.06
VCO+	28.2	25.48	29.61	38.21
Pd_PH3_2_C6H8	16.2	13.63	3.78	13.32
Pd_PH3_2_C10H12-b	17.3	13.37	-1.54	9.11
FeCl	80.5	80.06	78.94	84.77

MR-MGM-BE4				
CaO	96.15	97.05	104.45	124.23
LiO-	57.59	52.31	53.4	61.83
KO-	33.14	20.02	23.35	37.69
MgS	55.68	49.3	46.91	55.31
MR-MGN-BE17				
NF3	204.53	207.48	205.84	242.56
CO2	389.61	396.1	387.31	415.56
SiO (mult=1)	192.4	193.36	187.36	195.65
SO2	259.61	258.01	249.05	277.06
CO	259.42	260.68	254.73	268.3
SO (m=3)	125.69	127.79	125.43	139.57
ClO	64.84	65.25	64.92	79.92
F2	38.27	34.21	35.64	51.24
N2	228.48	222.76	229	242.97
O2	120.37	122.43	122.99	142.81
NO	152.7	149.81	154.72	171.75
CN	181.27	173.11	179.01	197.02
B2 -> 2B	67.4	63.85	60	76.91
O3 -> O2 + O	26.61	14.09	16.27	41.16
C2 -> 2C	146.88	131.28	119.22	93.61
S4 -> 2S2	25.75	20.14	12.86	28.35
Cl2O -> Cl2 + O	41.71	40.17	40.4	53.04
MR-TML-BE12				
TiCl	101.7	101.72	102.85	115.59
VF5	564.15	550.98	556.17	629.81
CrCl	90.15	92.31	85.85	88.91
CrOF	247.58	217.97	226.66	254.88
(FeBr2)2	366.8	361.73	340.4	369.41
Co(CO)4H	1230.13	1198.2	1189.67	1309.72
NiCH2+ -> Ni+ + CH2	76.3	63.35	73	90.82
Fe(CO)5 -> Fe + 5CO	147.4	86.07	122.18	193.05
VS -> V + S	106.9	99.21	102.4	128.27
CuCl	90.2	88.24	80.06	86.4
VO	151	141.91	151.06	182.06
NiCl	88.7	88.46	81.14	89.46
IsoL6/11				
10-	6.82	5.36	2.5	5.26
13-	33.52	32.34	30.32	31.06
14-	5.3	3.63	3.65	6.23
20-	4.66	4.56	4.29	4.9
3-	9.77	10	7.32	7.18
9-	21.76	20.59	18.07	17.65
IP23				

C	259.7	264.61	266.29	266.15
S	238.9	240.1	243.78	240.91
SH	238.9	240.14	241.4	239.28
Cl	299.1	300.2	301.1	298.91
Cl2	265.3	263.15	261.24	255.96
OH	299.1	304.09	306.32	304.59
O	313.9	317.46	326.8	324.72
O2	278.9	289.49	289.71	282.5
P	241.9	238.43	238.6	241.02
PH	234.1	232.98	234.27	236
PH2	226.3	225.93	228.84	229.94
S2	216	217.67	219.3	216.65
Si	187.9	184.44	186.99	188.92
Cr	156.01	157.03	164.6	170.5
Cu	178.17	180.56	190.21	193.05
FeC	173.71	177.63	184.55	186.78
Mo	163.71	161.54	167.12	172.08
Pd	192.24	189.41	196.4	200.16
Rh	172.11	169	177.68	180.38
Ru	169.86	167.6	175.28	178.88
Zn	216.63	219.42	221.66	221.22
Co	181.1	189.54	186.86	187.51
Sc	151.32	153.24	150.83	146.88
EA13/03				
C	29.1	30.48	31.19	35.75
S	47.9	49.03	50.56	49.6
SH	53.3	53.53	52.92	52.7
Cl	83.4	84.12	83.72	83.12
Cl2	55.6	57.83	64.57	59.76
OH	42.1	38.42	40.37	42.32
O	33.7	31.09	36.93	38.26
O2	10.8	7.24	11.98	8.83
P	17.2	18.23	22.01	20.16
PH	23.2	23.45	25.09	24.12
PH2	29.4	28.95	28.32	28.17
S2	38.5	37.54	38.65	36.19
Si	31.9	28.82	29.96	33.26
PA8				
NH3	211.9	209.85	211.27	210.89
H2O	171.8	170.17	170.46	170.39
C2H2	156.6	157.83	158.39	158.91
SiH4	156.5	156.11	157.4	157.01
PH3	193.1	190.58	193.11	190.24
H2S	173.7	172.23	174.82	174.38

HCl	137.1	136.06	138.01	138.93
H2	105.9	103.71	104.46	106.03
πTC13				
E2(propyne (C3H4))-E1(allene(C3H4))	-1.4	0.79	2.22	3.1
E4(penta-1,3-diyne(C5H4))-E3(penta-1,2,3,4-tetraene(C5H4))	-8.8	-5.34	-2.44	0.16
E6(penta-1,3,5-triyne(C7H4))-E5(hepta-1,2,3,4,5,6-haxaaene(C7H4))	-14.3	-9.73	-5.54	-1.42
P-2	167.81	167.53	168.17	167.91
P-4	193.45	193.98	198.46	196.42
P-6	209.68	211.15	216.27	214.26
P-8	219.67	222.04	227.61	225.72
P-10	225.95	229.76	235.68	233.96
SB-2	214.46	214.25	215.56	213.72
SB-4	226.15	227.85	229.97	228.25
SB-6	233.44	236.94	239.68	238.26
SB-8	238.16	243.17	246.46	245.34
SB-10	240.97	247.77	251.54	250.72
HTBH38/18 (forward and reverse reactions)				
H + HCl → H2 + Cl	6.1	3.94	-0.91	0.34
	8	6.91	4.43	-1.22
OH + H2 → H2O + H	5.2	5.02	0.88	-5.94
	21.6	20.6	13.2	13.53
CH3 + H2 → CH4 + H	11.9	11.87	8.9	4.02
	15	14.36	9.69	9.47
OH + CH4 → H2O + CH3	6.3	4.76	2.33	-5.2
	19.5	17.85	13.86	8.82
H + H2 → H2 + H	9.7	10.76	4.32	3.77
	9.7	10.76	4.32	3.77
OH + NH3 → H2O + NH2	3.4	1.69	-2.26	-11.55
	13.7	11.38	7.16	-0.85
HCl + CH3 → CH4 + Cl	1.8	-0.31	-1.29	-5.71
	6.8	5.15	4.84	-1.82
OH + C2H6 → H2O + C2H5	3.5	1.87	-0.7	-8.65
	20.4	19.3	15.48	10.65
F + H2 → HF + H	1.6	-1.25	-5.55	-12.43
	33.8	30.56	23.11	24.46
O + CH4 → OH + CH3	14.4	12.07	7.47	-0.06
	8.9	5.52	4.35	-0.64
H + PH3 → H2 + PH2	2.9	3.28	-0.94	-1.65
	24.7	25.7	23.17	18.38
H + HO → H2 + O	10.9	8.57	3.96	3.56
	13.2	12.64	6.29	-1.3
H + H2S → H2 + HS	3.9	3.83	-0.45	-1.13
	17.2	18.2	15.92	9.5

O + HCl → OH + Cl	10.4	7.07	1.44	-10.1
	9.9	5.98	4.44	-6.79
CH3 + NH2 → CH4 + NH	8.9	6.22	6.08	0.66
	22	21.35	17.36	10.83
C2H5 + NH2 → C2H6 + NH	9.8	7.73	8.17	2.86
	19.4	18.53	14.79	7.76
NH2 + C2H6 → NH3 + C2H5	11.3	9.71	8.82	1.52
	17.8	17.44	15.58	10.12
NH2 + CH4 → NH3 + CH3	13.9	12.46	11.39	4.51
	16.9	15.85	13.49	7.82
s-trans cis-C5H8 → s-trans cis-C5H8	39.7	38.91	39.01	31.43
	39.7	38.91	39.01	31.43
NHTBH38/18 (forward and reverse reactions)				
H + N2O → OH + N2	17.7	18.98	11.81	10.46
	82.6	79.45	73.12	52.84
H + FH → HF + H	42.1	41.98	31.83	27.98
	42.1	41.98	31.83	27.98
H + ClH → HCl + H	17.8	18.73	13.13	10.4
	17.8	18.73	13.13	10.4
H + FCH3 → HF + CH3	30.5	31.8	22.03	18.73
	56.9	55.72	48.71	41.14
H + F2 → HF + F	1.5	-0.05	-7.29	-9.59
	104.8	107.17	95.22	80
CH3 + FCl → CH3F + Cl	7.1	2.91	-1.53	-6.41
	59.8	57.54	51.24	41.95
F- + CH3F → FCH3 + F-	-0.6	-0.89	-3.94	-8.33
	-0.6	-0.89	-3.94	-8.33
F-···CH3F → FCH3···F-	13.4	14.43	9.98	6.66
	13.4	14.43	9.98	6.66
Cl- + CH3Cl → ClCH3 + Cl-	2.5	2.4	-0.53	-3.73
	2.5	2.4	-0.53	-3.73
Cl-···CH3Cl → ClCH3···Cl-	13.5	13.4	9.04	6.94
	13.5	13.4	9.04	6.94
F- + CH3Cl → FCH3 + Cl-	-12.3	-14.34	-16.49	-19.51
	19.8	21.42	18	12.09
F-···CH3Cl → FCH3···Cl-	3.5	3.02	0.09	-0.98
	29.6	31.33	26.23	21.04
OH- + CH3F → HOCH3 + F-	-2.7	-3.07	-5.93	-10.66
	17.6	18.52	14.55	9.63
OH-···CH3F → HOCH3···F-	11	11.96	7.38	3.37
	47.7	49.96	45.05	42.72
H + N2 → HN2	14.6	13.92	7.82	5.57
	10.9	11.54	10.96	9.24
H + CO → HCO	3.2	3.98	-0.56	-1.69

	22.8	23.16	24.65	24.72
H + C2H4 → CH3CH2	2	3.45	-0.07	-0.04
	42	43.28	41.87	40.39
CH3 + C2H4 → CH3CH2CH2	6.4	5.81	6.06	1.57
	33	32.79	29.4	29.72
HCN → HNC	48.1	46.19	47.7	45.95
	33	33.76	33.79	30.97
NCCE30/18				
(NH3)2	3.09	3.16	2.67	3.34
(HF)2	4.49	5.17	4.72	5
(H2O)2	4.91	5.44	4.96	5.44
NH3···H2O	6.38	6.49	6.32	7.15
(HCONH2)2	15.41	14.14	13.06	14.24
(HCOOH)2	17.6	16.35	15.17	16.33
C2H4···F2	1.06	1.52	1.5	3.17
NH3···F2	1.8	2.22	2.9	5.45
C2H2···ClF	3.79	4.77	3.79	6.18
HCN···ClF	4.8	5.19	4.57	5.93
NH3···Cl2	4.85	5.2	5.48	7.95
H2O···ClF	5.2	6.27	5.69	7.41
NH3···ClF	11.17	11.23	12.83	17.09
(H2S)2	1.62	1.51	0.9	1.8
(HCl)2	1.91	1.95	1.32	2.11
HCl···H2S	3.26	3.23	2.87	4.16
CH3Cl···HCl	3.39	3.5	2.21	3.39
HCN···CH3SH	3.58	3.6	2.57	3.52
CH3SH···HCl	4.74	4.77	3.77	5.61
CH4···Ne	0.18	0.32	0.02	0.27
C6H6···Ne	0.41	0.91	-0.11	0.35
(CH4)2	0.53	0.79	-0.5	0.01
CO2···Ar	0.57	0.59	-0.26	0.26
(C2H2)2	1.36	1.49	0.44	1
(C2H4)2	1.44	1.94	-0.48	0.36
sandwich (C6H6)2	1.65	2.14	-2.26	-1.56
T-shaped (C6H6)2	2.63	3.13	-0.21	0.11
parallel-displaced (C6H6)2	2.59	3.46	-1.82	-0.96
parallel-displaced(CO2)2	1.49	1.48	0.2	0.71
sandwich (C5H5N)2	2.89	2.77	-1.69	-0.19
NGD21				
He2	0.02	0.02	-0.04	0.06
Ne2	0.08	0.13	-0.06	0.12
Ar2	0.29	0.24	-0.22	0.11
Kr2	0.4	0.29	-0.32	0.09
HeNe	0.04	0.06	-0.05	0.09

HeAr	0.06	0.06	-0.08	0.09
NeAr	0.13	0.16	-0.1	0.13
HeHe_L_0.3A	0.01	0.01	-0.07	0.07
HeHe_R_0.3A	0.02	0.01	-0.03	0.04
ArAr_L_0.3A	0.14	0.11	-0.57	-0.18
ArAr_R_0.3A	0.24	0.19	-0.11	0.14
NeNe_L_0.3A	0.01	0.14	-0.16	0.04
NeNe_R_0.3A	0.07	0.07	-0.04	0.1
KrKr_L_0.3A	0.24	0.1	-0.79	-0.29
KrKr_R_0.3A	0.34	0.25	-0.16	0.16
HeNe_L_0.3A	0.01	0.07	-0.1	0.08
HeNe_R_0.3A	0.03	0.03	-0.03	0.06
HeAr_L_0.3A	0.02	0.05	-0.15	0.06
HeAr_R_0.3A	0.05	0.04	-0.05	0.07
NeAr_L_0.3A	0.05	0.15	-0.25	0.02
NeAr_R_0.3A	0.11	0.1	-0.06	0.11
AE17				
H	-0.5	-0.5	-0.5	-0.5
He	-2.9	-2.91	-2.92	-2.89
Li	-7.48	-7.48	-7.49	-7.46
Be	-14.67	-14.66	-14.67	-14.63
B	-24.65	-24.64	-24.67	-24.61
C	-37.85	-37.83	-37.86	-37.8
N	-54.59	-54.58	-54.61	-54.54
O	-75.07	-75.06	-75.1	-75.01
F	-99.73	-99.73	-99.78	-99.68
Ne	-128.94	-128.94	-128.98	-128.87
Na	-162.25	-162.26	-162.3	-162.17
Mg	-200.05	-200.07	-200.1	-199.95
Al	-242.35	-242.35	-242.4	-242.24
Si	-289.36	-289.36	-289.4	-289.23
P	-341.26	-341.25	-341.29	-341.12
S	-398.11	-398.11	-398.15	-397.95
Cl	-460.15	-460.15	-460.18	-459.98
HC7/11				
E22-E1	14.34	20.79	-1.12	13.78
E31-E1	25.02	27.88	1.22	18.42
octane iso	1.9	2.48	-7.98	-5.18
DE (rxn a)	9.81	8.16	4.6	5.78
DE (rxn b)	14.84	12.18	6.81	8.59
DE (rxn c)	193.99	196.22	162.96	193
DE (rxn d)	127.22	127.44	103.03	124.9
3dEE8				
Sc	32.94	32.47	20.15	13.31

Mn+	27.08	17.68	21.9	26.57
Fe	34.24	39.94	22.43	21.27
Ni+	24	19.17	17.88	24.19
Zn	92.38	100.65	97.71	96.83
Ca+	39.03	29.24	27.42	24.22
V	6.04	4.14	-0.51	-12.19
Fe2	12.22	33.2	-3.65	11.29
4dAEE5				
Mo+	43.46	37.7	27.81	32.9
Ru+	26.17	27.93	28.12	24
Rh+	23.34	16.79	16.54	16.47
Pd	18.77	15.9	13.81	15.8
Y+	2.4	4.89	0.49	-1.43
pAEE5				
F	292.79	299.51	295.11	293.46
Ar	266.31	272.74	262.87	261.4
C+	122.95	122.31	122.56	114.15
Al	82.97	89.13	88.37	82.86
Si+	126.03	128.4	127.69	121.87
DC9/18				
HCN···BF3 → HCN+BF3	5.7	6.12	3.77	4.33
C6Cl6+6HCl→6Cl2+C6H6	152.6	147.59	127.04	135.99
P4→4P	289.9	305.09	278.5	308.07
SF6→S+6F	477.5	484.57	448.85	501.88
PF5→P+5F	556.4	564.67	532.84	562
P4O10→P4+5O2	719.7	711.06	648.74	618.57
C6F6→6C+6F	1388.1	1420.41	1378.37	1484.52
Si(OCH3)4→Si+4C+4O+12H	2023.5	2033.95	2003.85	2045.58
urotropin→6C+4N+12H	2151.1	2148.01	2129.06	2213.89
2pIsoE4				
C	3.8	3.63	0.78	1.45
N	57.1	62.55	69.78	64.37
O	9.9	9.8	10.78	9.43
F	26.9	28.81	24.72	26.06
4pIsoE4				
As	33	37.36	44.65	37.9
Br	-6.3	-6.27	-7.65	-5.22
Ge	24.6	21.69	22.89	22.73
Se	20.8	23.11	23.03	22.67
SMAE3				
SO3	344.23	343.59	329.24	370.34
H2S2	240.78	244.59	236.55	244.52
H2SO4	602.18	596.56	578.04	621.67
TMD-BE7				

Ag2	38.3	39.15	35.36	40.73
Cu2	47.2	44.65	41.04	47.98
CuAg	40.7	39.43	38.18	44.3
Zr2	70.8	54.12	56.6	84.99
Fe2	26.59	15.65	9.36	41.22
Cr2	36	-23.66	-3.27	32.4
V2	64.2	4.44	37.41	102.2

[a]For details of all the species in the πTC13 database, please see Ref. (96).
[b]The notations _L_0.3Å and _R_0.3Å imply 0.3 Å to the left and 0.3 Å to the right, respectively, of the equilibrium distance of the potential energy curve of inert gas dimers.
[c]For details of all the species in HC7/11 database, please see Ref. (78).
[d]For details of the educts and products of 10-, 13-, 14-, 20-, 3-, and 9-, please see Ref. (138).

Table S23. The geometries of systems whose geometries are not in the SI of the GAM functional paper

TMD-BE7/3dEE8

Fe_2 (septet)

0 7			
Fe	0.0000000	0.0000000	0.0000000
Fe	0.0000000	0.0000000	2.0200000

Fe_2 (nonet)

0 9			
Fe	0.0000000	0.0000000	0.0000000
Fe	0.0000000	0.0000000	2.0200000

NCCE30/18

CH_3SH-HCl (It was not given in the Supplementary Material of the GAM paper[8].)

0 1			
C	-1.4476480	1.1556490	0.018513
S	-1.4145950	- 0.6598460	-0.083544
H	-1.4662840	1.5168160	-1.009880
H	-0.5529710	1.5352650	0.510012
H	-2.3442390	1.4977330	0.531863
H	-1.3773610	-0.8909210	1.238214
Cl	2.1257660	0.0240810	0.003156
H	0.9222380	-0.4446350	-0.098247

SMAE3

SO_3

0 1			
S	0.0000000	0.0000000	0.0000000
O	0.0000000	0.0000000	1.4232900
O	1.232605294	0.0000000	-0.7116450
O	-1.232605294	0.0000000	-0.711645

H_2S_2

0 1			
S	0.0000000	1.0282000	-0.0552000
S	0.0000000	-1.0282000	-0.0552000
H	0.9425000	1.2122000	0.8824000
H	-0.9425000	-1.2122000	0.8824000

H_2SO_4

0 1			
S	0.0000000	0.0000000	0.1248000
O	1.2510000	-0.0349000	0.8000000

O	-1.2510000	0.0349000	0.8000000
O	0.0000000	-1.2172000	-0.8732000
O	0.0000000	1.2172000	-0.8732000
H	-0.3548000	1.9933000	-0.4121000
H	0.3548000	-1.9933000	-0.4121000

5. Addional figures

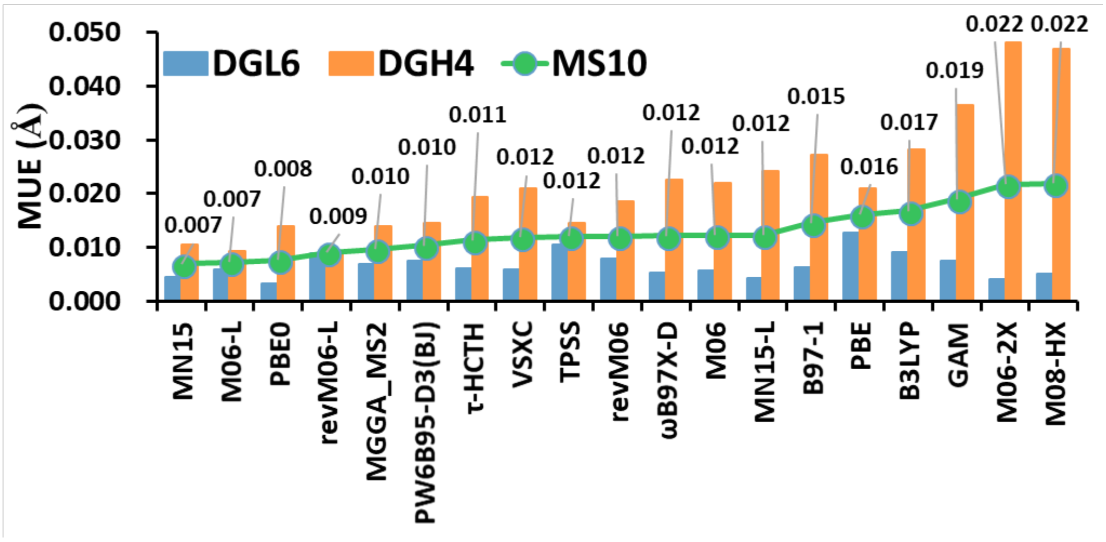

Fig. S1. The MUEs (in Å) for the molecular structure subdatabases.

The basis set for HBr, ZnS, and NaBr are changed from 6-311+G(2df,2p) to aug-cc-pVQZ for H, Zn, and S, B2 for Zn, cc-pwCVQZ-DK for Br.

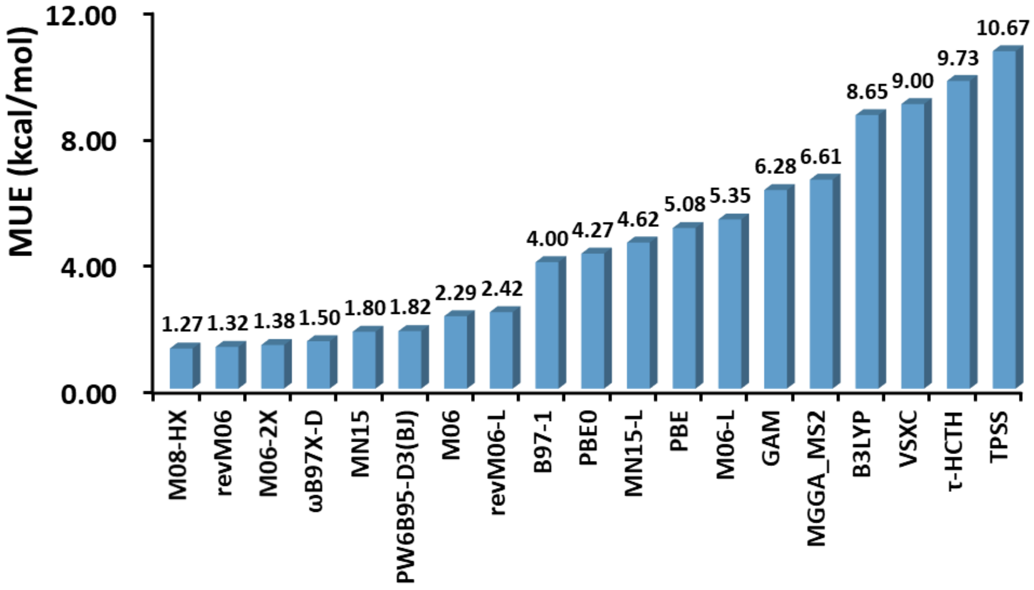

Fig. S2. The MUEs (in kcal/mol) for the alkyl bond dissociation energy (ABDE13) database.

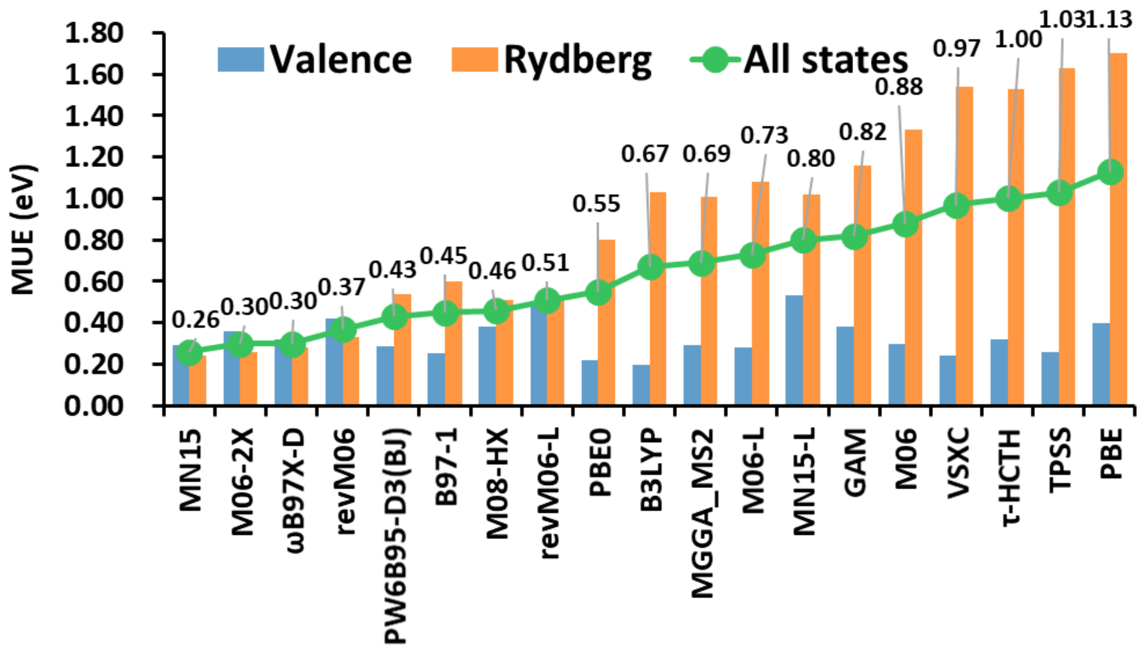

Fig. S3. The MUEs (in eV) of 12 selected functionals for the vertical excitation energies of 30 valence, 39 Rydberg, and all 69 transitions.

The labels represent the values of average MUEs for the EE69 database.

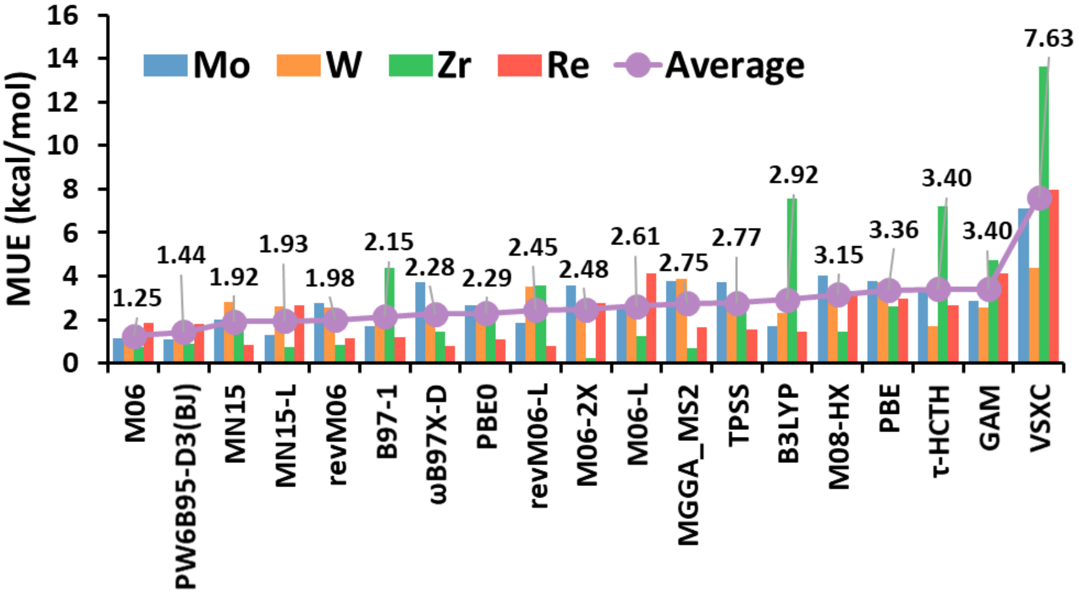

Fig. S4. The MUEs (kcal/mol) of transition-metal reaction barrier height (TMBH22) database.

There are respectively 6, 7, 4, and 5 reactions in the database for Mo, W, Zr and Re reaction barrier heights. The results of TPSS, M08-HX, τ-HCTH, VSXC, MGGA_MS2, PW6B95-D3(BJ), B97-1, and revM06 are calculated in the present paper. The revM06-L and ωB97X-D results are from ref. (1). The MN15, MN15-L, and GAM results are from ref. (10). The results for Mo and W of MN15, MN15-L, GAM, revM06-L, and ωB97X-D are recalculated in the present study as the number of reactions changed. All other results are from refs. (57-59).

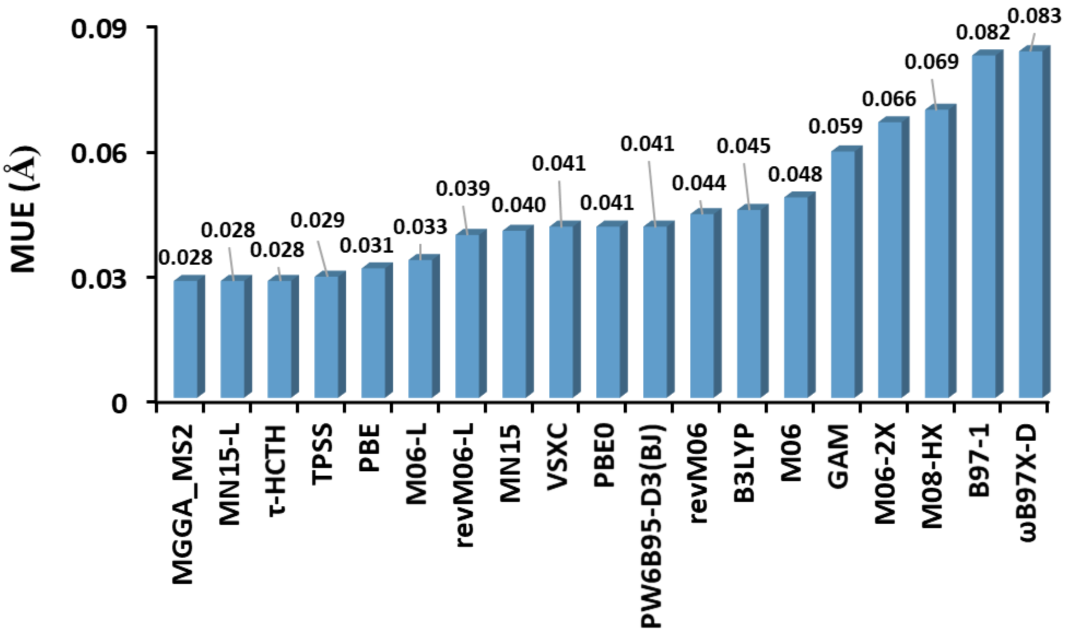

Fig. S5. The MUEs (Å) of equilibrium bond lengths for homonuclear transition metal dimers (database TMDBL7).

The bond lengths of MN15, MN15-L, ωB97X-D, PBE, B3LYP, M08-HX, TPSS, τ-HCTH, VSXC, PBE0, revM06, M06 and M06-2X are calculated in the present study using the LANL2DZ basis set. The results with other functionals are from refs. (1, 10, 63).

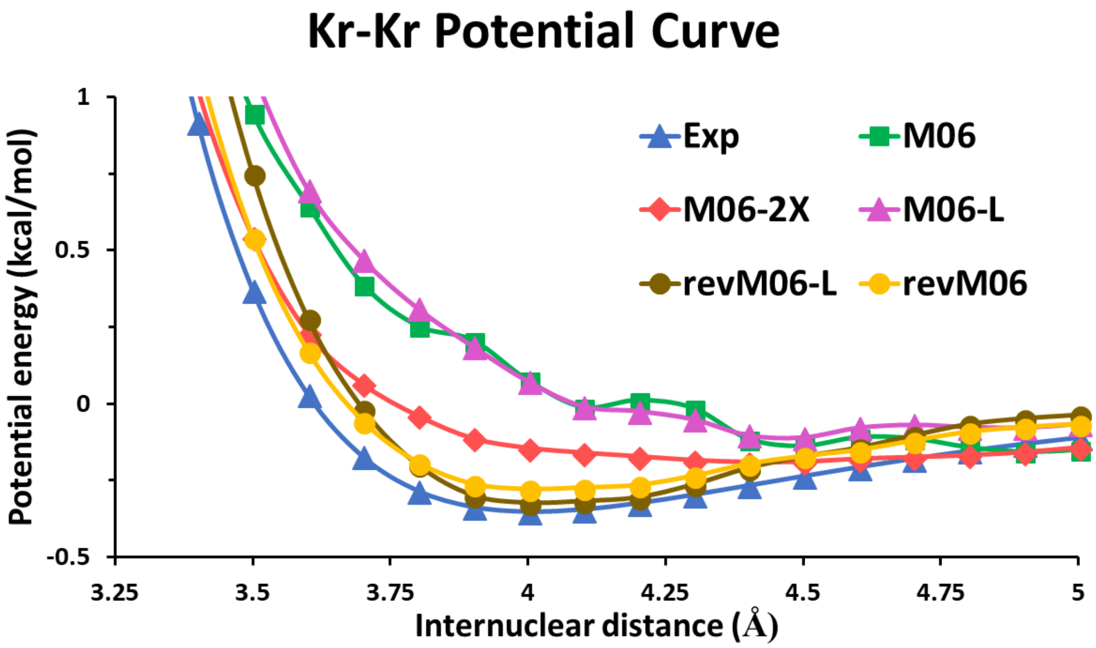

Fig. S6. Kr-Kr potential curve.

The data are calculated by revM06-L, M06-L, revM06, M06, and M06-2X with the (99, 590) grid and the aug-cc-pVQZ basis set and compared to the experimental curve. The basis set superposition errors were corrected for all calculations. Note that counterpoise corrections are included in Fig. 4 and in the present figure, but all other results in the article and the SI Appendix are calculated without counterpoise corrections.

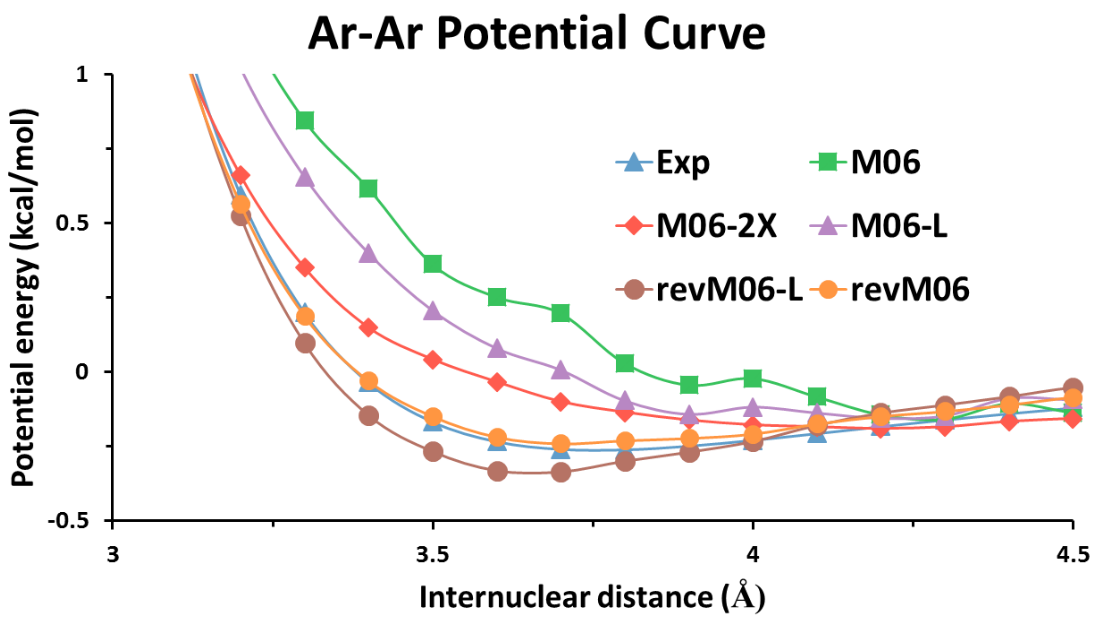

Fig. S7. Ar-Ar potential curve.

The data are calculated by revM06-L, M06-L, revM06, M06, and M06-2X with the (99, 590) grid and the aug-cc-pVQZ basis set and compared to the experimental curve. The basis set superposition errors were not corrected. This figure may be compared to Fig. 4.

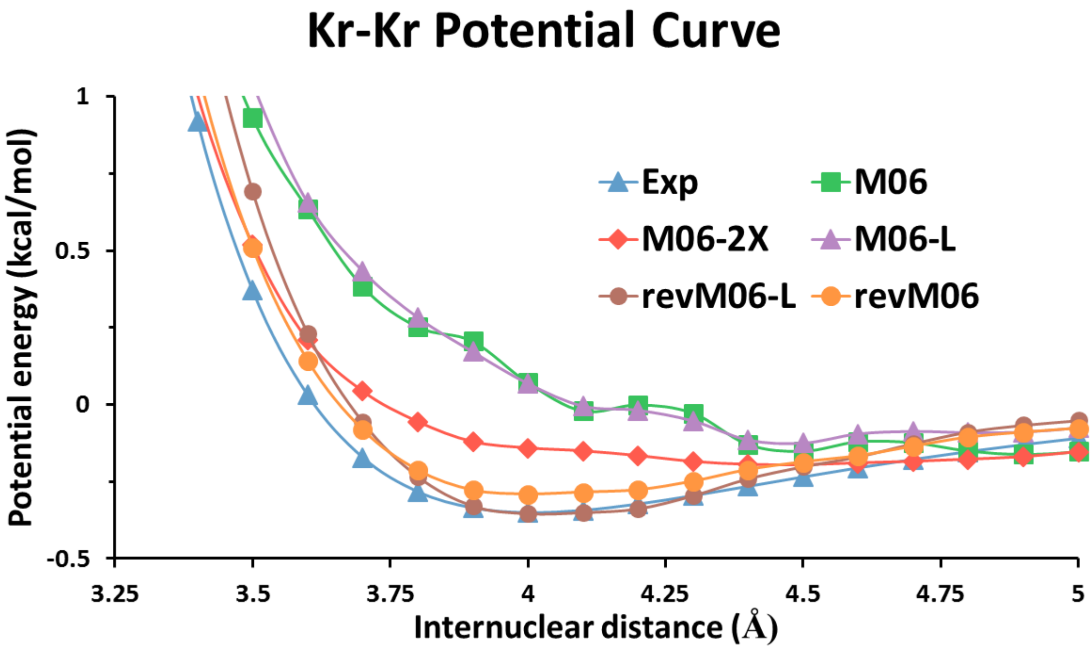

Fig. S8. Kr-Kr potential curve.

The data are calculated by revM06-L, M06-L, revM06, M06, and M06-2X with the (99,590) grid and the aug-cc-pVQZ basis set and compared to the experimental curve. The basis set superposition errors were not corrected. This figure may be compared to Fig. S6.

6. References cited in this SI Appendix

1. Wang Y, Jin XS, Yu HS, Truhlar DG, He X (2017) Revised M06-L functional for improved accuracy on chemical reaction barrier heights, noncovalent interactions, and solid-state physics. *Proc Natl Acad Sci USA* 114:8487-8492.
2. Van Voorhis T, Scuseria GE (1998) A novel form for the exchange-correlation energy functional. *J Chem Phys* 109:400-410.
3. Zhao Y, Schultz NE, Truhlar DG (2005) Exchange-correlation functional with broad accuracy for metallic and nonmetallic compounds, kinetics, and noncovalent interactions. *J Chem Phys* 123:188-192.
4. Perdew JP, Burke K, Ernzerhof M (1996) Generalized gradient approximation made simple. *Phys Rev Lett* 77:3865-3868.
5. Stoll H, Pavlidou CME, Preuss H (1978) On the calculation of correlation energies in the spin-density functional formalism. *Theo Chem Acc* 49:143-149.
6. Becke AD (1998) A new inhomogeneity parameter in density functional theory. *J Chem Phys* 109:2092-2098.
7. Zhao Y, Schultz NE, Truhlar DG (2006) Design of density functionals by combining the method of constraint satisfaction with parametrization for thermochemistry, thermochemical kinetics, and noncovalent interactions. *J Chem Theory Comput* 2:364-382.
8. Yu HS, He X, Truhlar DG (2016) MN15-L: A new local exchange-correlation functional for Kohn–Sham density functional theory with broad accuracy for atoms, molecules, and solids. *J Chem Theory Comput* 12:1280-1293.
9. Yu HS, Zhang WJ, Verma P, He X, Truhlar DG (2015) Nonseparable exchange-correlation functional for molecules, including homogeneous catalysis involving transition metals. *Phys Chem Chem Phys* 17:12146-12160.
10. Yu HS, He X, Li SL, Truhlar DG (2016) MN15: A Kohn–Sham global-hybrid exchange–correlation density functional with broad accuracy for multi-reference and single-reference systems and noncovalent interactions. *Chem Sci* 7:5032-5051.
11. Voorhis TV, Scuseria GE (1998) A novel form for the exchange-correlation energy functional. *J Chem Phys* 109:400-410.
12. Goerigk L*, et al.* (2017) A look at the density functional theory zoo with the advanced GMTKN55 database for general main group thermochemistry, kinetics and noncovalent interactions. *Phys Chem Chem Phys* 19:32184-32215.
13. Pernal K, Podeszwa R, Patkowski K, Szalewicz K (2009) Dispersionless density functional theory. *Phys Rev Lett* 103:263201.
14. Anonymous (Jan. 30. 2018) https://physics.nist.gov/PhysRefData/Handbook/periodictable.htm.
15. Moore CE (1948) *Atomic Energy Levels* (National Bureau of Standards: Washington).
16. Cheng L, Gauss J, Ruscic B, Armentrout PB, Stanton JF (2017) Bond dissociation energies for diatomic molecules containing 3d transition metals: Benchmark scalar-relativistic coupled-cluster calculations for twenty molecules. *J Chem Theory Comput* 13:1044-1056.
17. Fang Z, Vasiliu M, Peterson KA, Dixon DA (2017) Prediction of bond dissociation energies/heat of formation for diatomic transition metal compounds: CCSD(T) works.

J Chem Theory Comput 13:1057-1066.
18. Berning A, Schweizer M, Werner HJ, Knowles P, Palmieri P (2000) Spin-orbit matrix elements for internally contracted multireference configuration interaction wavefunctions. *Mol Phys* 98:1823-1833.
19. Werner H-J*, et al.* (*Molpro,* version 2010.1. :http://www.molpro.net.
20. Docken KK, Hinze J (1972) LiH potential curves and wavefunctions for X $^1\Sigma^+$, A $^1\Sigma^+$, B $^1\Pi$, $^3\Sigma^+$, and $^3\Pi$. *J Chem Phys* 57:4928-4936.
21. Ruedenberg K, Cheung LM, Elbert ST (1979) MCSCF optimization through combined use of natural orbitals and the Brillouin–Levy–Berthier theorem. *Int J Quantum Chem* 16:1069-1101.
22. Roos BO (1980) The complete active space SCF method in a Fock-matrix-based super-CI formulation. *Int J Quantum Chem* 14:175-189.
23. Werner HJ, Meyer WA (1981) A quadratically convergent MCSCF method for the simultaneous optimization of several states. *J Chem Phys* 74:5794-5801.
24. Ruedenberg K, Schmidt MW, Gilbert MM, Elbert ST (1982) Are atoms intrinsic to molecular electronic wavefunctions? I. The FORS model. *Chem Phys* 71:41-49.
25. Werner HJ, Knowles PJ (1985) A second order multiconfiguration SCF procedure with optimum convergence. *J Chem Phys* 82:5053-5061.
26. Knowles PJ, Werner HJ (1985) An efficient second-order MCSCF method for long configuration expansions. *Chem Phys Lett* 115:259-267.
27. Dunning THJ (1989) Gaussian basis sets for use in correlated molecular calculations. I. The atoms Boron through neon and hydrogen. *J Chem Phys* 90:1007-1023.
28. Balabanov NB, Peterson KA (2006) Basis set limit electronic excitation energies, ionization potentials, and electron affinities for the 3d transition metal atoms: coupled cluster and multireference methods. *J Chem Phys* 125:074110.
29. Gagliardi L, Roos BO (2003) The electronic spectrum of $Re_2Cl_8^{2-}$: A theoretical study. *Inorg Chem* 42:1599-1603.
30. Gagliardi L, Heaven MC, Krogh JW, Roos BO (2005) The electronic spectrum of the UO_2 molecule. *J Am Chem Soc* 127:86-91.
31. Roos BO, Malmqvist P-Å, Gagliardi L (2006) Exploring the actinide-actinide bond: Theoretical studies of the chemical bond in Ac_2, Th_2, Pa_2, and U_2. *J Am Chem Soc* 128:1700-1706.
32. Zhao Y*, et al.* (2017) MN-GFM, version 6.8: Minnesota Gaussian Functional Module. *University of Minnesota: Minneapolis, MN.*
33. Frisch MJ*, et al.* (2009) Gaussian 09, Revision C.01. *Gaussian, Inc.*
34. Posada-Borbón A, Posada-Amarillas A (2014) Theoretical DFT study of homonuclear and binary transition-metal dimers. *Chem Phys Lett* 618:66–71.
35. Anonymous (http://cccbdb.nist.gov/expbondlengths1.asp,accessed on Oct. 29, 2014.
36. Anonymous (http://webbook.nist.gov/cgi/cbook.cgi?ID=C7664939&Units=SI&Mask=1#Thermo-Gas, accessed on Jul. 26, 2015.
37. Anonymous (http://webbook.nist.gov/cgi/cbook.cgi?ID=C63344865&Units=SI, accessed on Jul. 26, 2015.
38. Anonymous (http://webbook.nist.gov/cgi/cbook.cgi?ID=C7446119&Units=SI,

accessed on Jul. 26, 2015.

39. Schwabe T (2014) An isomeric reaction benchmark set to test if the performance of state-of-the-art density functionals can be regarded as independent of the external potential. *Phys Chem Chem Phys* 16:14559-14567.
40. Yang K, Peverati R, Truhlar DG, Valero R (2011) Density functional study of multiplicity-changing valence and Rydberg excitations of p-block elements: Delta self-consistent field, collinear spin-flip time-dependent density functional theory (DFT), and conventional time-dependent DFT. *J Chem Phys* 135:044118.
41. Luo S, Truhlar DG (2012) How evenly can approximate density functionals treat the different multiplicities and ionization states of 4d transition metal atoms? *J Chem Theory Comput* 8:4112-4126.
42. Luo S, Averkiev B, Yang KR, Xu X, Truhlar DG (2014) Density functional theory of open-shell systems. the 3d-series transition-metal atoms and their cations. *J Chem Theory Comput* 10:102-121.
43. Tang KT, Toennies JP (2003) The van der Waals potentials between all the rare gas atoms from He to Rn. *J Chem Phys* 118:4976-4983.
44. Marshall MS, Burns LA, Sherrill CD (2011) Basis set convergence of the coupled-cluster correction, δ(MP2)(CCSD(T)): best practices for benchmarking non-covalent interactions and the attendant revision of the S22, NBC10, HBC6, and HSG databases. *J Chem Phys* 135:194102.
45. Mcmahon JD, Lane JR (2011) Explicit correlation and basis set superposition error: the structure and energy of carbon dioxide dimer. *J Chem Phys* 135:2836-2843.
46. de Lange KM, Lane JR (2011) Explicit correlation and intermolecular interactions: investigating carbon dioxide complexes with the CCSD(T)-F12 method. *J Chem Phys* 134:123-127.
47. Peverati R, Truhlar DG (2014) Quest for a universal density functional: the accuracy of density functionals across a broad spectrum of databases in chemistry and physics. *Phil Trans R Soc A* 372:20120476.
48. Yu H, Truhlar DG (2015) Components of the bond energy in polar diatomic molecules, radicals, and ions formed by group-1 and group-2 metal atoms. *J Chem Theory Comput* 11:2968-2983.
49. Zhang W, Truhlar DG, Tang M (2013) Tests of exchange-correlation functional approximations against reliable experimental data for average bond energies of 3d transition metal compounds. *J Chem Theory Comput* 9:3965-3977.
50. Averkiev BB, Zhao Y, Truhlar DG (2010) Binding Energy of d^{10} transition metals to alkenes by wave function theory and density functional theory. *J Mol Catal A* 324:80–88.
51. Xu X, Zhang W, Tang M, Truhlar DG (2015) Do practical standard coupled cluster calculations agree better than Kohn-Sham calculations with currently available functionals when compared to the best available experimental data for dissociation energies of bonds to 3d transition metals? *J Chem Theory Comput* 11:2036-2052.
52. Hoyer CE, Manni GL, Truhlar DG, Gagliardi L (2014) Controversial electronic structures and energies of Fe_2, Fe_2^+, and Fe_2^- resolved by RASPT2 calculations. *J Chem Phys* 141:204309-204309.

53. Vydrov OA, Van VT (2012) Benchmark assessment of the accuracy of several van der Waals density functionals. *J Chem Theory Comput* 8:1929-1934.
54. Li X, Xu X, You X, Truhlar DG (2016) Benchmark calculations for bond dissociation enthalpies of unsaturated methyl esters and the bond dissociation enthalpies of methyl linolenate. *J Phys Chem A* 120:4025-4036.
55. Řezáč J, Riley KE, Hobza P (2011) S66: A well-balanced database of benchmark interaction energies relevant to biomolecular structures. *J Chem Theory Comput* 7:2427-2438.
56. Isegawa M, Peverati R, Truhlar DG (2012) Performance of recent and high-performance approximate density functionals for time-dependent density functional theory calculations of valence and Rydberg electronic transition energies. *J Chem Phys* 137:75-87.
57. Hu L, Chen H (2015) Assessment of DFT methods for computing activation energies of Mo/W-mediated reactions. *J Chem Theory Comput* 11:4601-4614.
58. Sun Y, Chen H (2013) Performance of density functionals for activation energies of Zr-mediated reactions. *J Chem Theory Comput* 9:4735-4743.
59. Sun Y, Chen H (2014) Performance of density functionals for activation energies of Re-catalyzed organic reactions. *J Chem Theory Comput* 10:579–588.
60. Husch T, Freitag L, Reiher M (2018) Calculation of Ligand Dissociation Energies in Large Transition-Metal Complexes. *J Chem Theory Comput* 14:2456-2468.
61. Weymuth T, Couzijn EP, Chen P, Reiher M (2014) New benchmark set of transition-metal coordination reactions for the assessment of density functionals. *J Chem Theory Comput* 10:3092-3103.
62. Schultz NE, Zhao Y, Truhlar DG (2005) Density functionals for inorganometallic and organometallic chemistry. *J Phys Chem A* 109:11127-11143.
63. Tishchenko O, Zheng J, Truhlar DG (2008) Multireference model chemistries for thermochemical kinetics. *J Chem Theory Comput* 4:1208-1219.
64. Zhao Y*, et al.* (2009) Thermochemical Kinetics for Multireference Systems: Addition Reactions of Ozone. *J Phys Chem A* 113:5786-5799.
65. Fast PL, Corchado J, Sanchez ML, Truhlar DG (1999) Optimized parameters for scaling correlation energy. *J Phys Chem A* 103:3139-3143.
66. Lynch BJ, Zhao Y, Truhlar DG (2005) The 6-31B(d) basis set and the BMC-QCISD and BMC-CCSD multicoefficient correlation methods. *J Phys Chem A* 109:1643-1649.
67. Xu X, Zhang W, Tang M, Truhlar DG (2015) Do practical standard coupled cluster calculations agree better than Kohn-Sham calculations with currently available functionals when compared to the best available experimental data for dissociation energies of bonds to 3d transition metals? *J Chem Theory Comput* 11:2036.
68. Yamada C, Fujitake M, Hirota E (1989) Detection of the NaO radical by microwave spectroscopy. *J Chem Phys* 90:3033-3037.
69. Marenich AV, Boggs JE (2005) A model spin-vibronic Hamiltonian for twofold degenerate electron systems: A variational ab initio study of $\tilde{X}_2E$ CH_3O•. *J Chem Phys* 122:024308.
70. Herzberg G (1950) *Molecular structure and molecular spectra. I. spectra of diatomic molecules; 2nd ed* (D. Van Nostrand: Princeton) p 504.

71. Becke AD, Roussel MR (1989) Exchange holes in inhomogeneous systems: A coordinate-space model. *Phys Rev A* 39:3761-3767.
72. Kohn W, Sham LJ (1965) Self-consistent equations including exchange and correlation effects. *Phys Rev* 140:A1133-A1138.
73. Gáspár R (1954) Über eine approximation des Hartree-Fock schen potentials durch eine universelle potential function. *Acta Phys Hung* 3:263-286.
74. Gáspár R (1974) Statistical exchange for electron in shell and the Xα method. *Acta Phys Hung* 35:213-218.
75. Vosko SH, Wilk L, Nusair M (1980) Accurate spin-dependent electron liquid correlation energies for local spin density calculations: a critical analysis. *Can J Phys* 58:1200-1211.
76. Zhao Y, Truhlar DG (2008) Construction of a generalized gradient approximation by restoring the density-gradient expansion and enforcing a tight Lieb-Oxford bound. *J Chem Phys* 128:184109.
77. Perdew JP*, et al.* (2008) Restoring the density-gradient expansion for exchange in solids and surfaces. *Phys Rev Lett* 101:136406.
78. Peverati R, Zhao Y, Truhlar DG (2011) Generalized gradient approximation that recovers the second-order density-gradient expansion with optimized across-the-board performance. *J Phys Chem Lett* 2:1991-1997.
79. Becke AD (1986) Density functional calculations of molecular bond energies. *J Chem Phys* 84:4524-4529.
80. Perdew JP (1986) Density-functional approximation for the correlation energy of the inhomogeneous electron gas. *Phys Rev B* 33:8822-8824.
81. Lee C, Yang W, Parr RG (1988) Development of the Colle-Salvetti correlation-energy formula into a functional of the electron density. *Phys Rev B* 37:785-789.
82. Perdew JP (1991) *Electronic Structure of Solids' 9* (Ziesche, P., Eschrig, H., Eds, Berlin).
83. Adamo C, Barone V (1998) Exchange functionals with improved long-range behavior and adiabatic connection methods without adjustable parameters: The mPW and mPW1PW models. *J Chem Phys* 108:664-675.
84. Zhang Y, Yang W (1997) Comment on "Generalized gradient approximation made simple". *Phys Rev Lett* 80:890.
85. Hammer B (1999) Improved adsorption energetics within density-functional theory using revised Perdew-Burke-Ernzerhof functionals. *Phys Rev B* 59:7413-7421.
86. Boese AD, Handy NC (2001) A new parametrization of exchange–correlation generalized gradient approximation functionals. *J Chem Phys* 114:5497-5503.
87. Handy N, Cohen A (2001) Left-right correlation energy. *Mol Phys* 99:403-412.
88. Hoe WM, Cohen AJ, Handy NC (2001) Assessment of a new local exchange functional OPTX. *Chem Phys Lett* 341:319-328.
89. Dahlke EE, Truhlar DG (2005) Improved density functionals for water. *J Phys Chem B* 109:15677-15683.
90. Grimme S (2006) Semiempirical GGA-type density functional constructed with a long-range dispersion correction. *J Comput Chem* 27:1787-1799.
91. Zhao Y, González-García N, Truhlar DG (2005) Benchmark database of barrier

heights for heavy atom transfer, nucleophilic substitution, association, and unimolecular reactions and its use to test theoretical methods. *J Phys Chem A* 109:2012-2018.
92. Thakkar AJ, Mccarthy SP (2009) Toward improved density functionals for the correlation energy. *J Chem Phys* 131:134109.
93. Peverati R, Truhlar DG (2012) Exchange-correlation functional with good accuracy for both structural and energetic properties while depending only on the density and Its gradient. *J. Chem. Theory Comput.* 8:2310-2319.
94. Boese AD, Handy NC (2002) New exchange-correlation density functionals: The role of the kinetic-energy density. *J Chem Phys* 116:9559-9569.
95. Tao J, Perdew JP, Staroverov VN, Scuseria GE (2003) Climbing the density functional ladder: Nonempirical meta-generalized gradient approximation designed for molecules and solids. *Phys Rev Lett* 91:146401.
96. Zhao Y, Truhlar DG (2006) A new local density functional for main-group thermochemistry, transition metal bonding, thermochemical kinetics, and noncovalent interactions. *J Chem Phys* 125:194101.
97. Perdew JP, Ruzsinszky A, Csonka GI, Constantin LA, Sun J (2009) Workhorse semilocal density functional for condensed matter physics and quantum chemistry. *Phys Rev Lett* 103:026403.
98. Peverati R, Truhlar DG (2011) M11-L: A local density functional that provides improved accuracy for electronic structure calculations in chemistry and physics. *J Phys Chem Lett* 3:117-124.
99. Sun J*, et al.* (2013) Semilocal and hybrid meta-generalized gradient approximations based on the understanding of the kinetic-energy-density dependence. *J Chem Phys* 138:044113.
100. Peverati R, Truhlar DG (2012) An improved and broadly accurate local approximation to the exchange-correlation density functional: the MN12-L functional for electronic structure calculations in chemistry and physics. *Phys Chem Chem Phys* 14:13171-13174.
101. Roothaan CCJ (1951) New developments in molecular orbital theory. *Rev Mod Phys* 23:69-89.
102. Becke AD (1993) Density‐functional thermochemistry. III. The role of exact exchange. *J Chem Phys* 98:5648-5653.
103. Stephens PJD, Devlin FJC, Chabalowski CFN, Frisch MJJ (1993) Ab Initio calculation of vibrational absorption and circular dichroism spectra using density functional force fields. *J Phys Chem* 98:247-257.
104. Adamo C, Barone V (1999) Toward reliable density functional methods without adjustable parameters: The PBE0 model. *J Chem Phys* 110:6158-6170.
105. Becke AD (1996) Density‐functional thermochemistry. IV. A new dynamical correlation functional and implications for exact‐exchange mixing. *J Chem Phys* 104:1040-1046.
106. Adamo C, Barone V (1997) Toward reliable adiabatic connection models free from adjustable parameters. *Chem Phys Lett* 274:242-250.
107. Schmider HL, Becke AD (1998) Optimized density functionals from the extended G2

test set. *J Chem Phys* 108:9624-9631.

108. Hamprecht FA, Cohen AJ, Tozer DJ, Handy NC (1998) Development and assessment of new exchange-correlation functionals. *J Chem Phys* 109:6264-6271.
109. Lynch BJ, Fast PL, Maegan Harris A, Truhlar DG (2000) Adiabatic connection for kinetics. *J Phys Chem A* 104:4811-4815.
110. Wilson PJ, Bradley TJ, Tozer DJ (2001) Hybrid exchange-correlation functional determined from thermochemical data and ab initio potentials. *J Chem Phys* 115:9233-9242.
111. Reiher M, Salomon O, Hess BA (2001) Reparameterization of hybrid functionals based on energy differences of states of different multiplicity. *Theo Chem Acc* 107:48-55.
112. Xu X, Goddard Ⅲ WA (2004) The X3LYP extended density functional for accurate descriptions of nonbond interactions, spin states, and thermochemical properties. *Proc Natl Acad Sci USA* 101:2673-2677.
113. Zhao Y, Truhlar DG (2004) Hybrid meta density functional theory methods for thermochemistry, thermochemical kinetics, and noncovalent interactions: The MPW1B95 and MPWB1K models and comparative assessments for hydrogen bonding and van der Waals interactions. *J Phys Chem A* 108:6908-6918.
114. Keal TW, Tozer DJ (2005) Semiempirical hybrid functional with improved performance in an extensive chemical assessment. *J Chem Phys* 123:121103.
115. Peverati R, Truhlar DG (2011) Communication: A global hybrid generalized gradient approximation to the exchange-correlation functional that satisfies the second-order density-gradient constraint and has broad applicability in chemistry. *J Chem Phys* 135:191102.
116. Yanai T, Tew DP, Handy NC (2004) A new hybrid exchange-correlation functional using the Coulomb-attenuating method (CAM-B3LYP). *Chem Phys Lett* 393:51-57.
117. Heyd J, Scuseria GE, Ernzerhof M (2003) Hybrid functionals based on a screened Coulomb potential. *J Chem Phys* 118:8207-8215.
118. Henderson TM, Izmaylov AF, Scalmani G, Scuseria GE (2009) Can short-range hybrids describe long-range-dependent properties? *J Chem Phys* 131:225-229.
119. Henderson TM, Izmaylov AF, Scuseria GE, Savin A (2008) Assessment of a middle-range hybrid functional. *J Chem Theory Comput* 4:1254.
120. Chai JD, Head-Gordon M (2008) Systematic optimization of long-range corrected hybrid density functionals. *J Chem Phys* 128:57-63.
121. Peverati R, Truhlar DG (2012) Screened-exchange density functionals with broad accuracy for chemistry and solid-state physics. *Phys Chem Chem Phys* 14:16187-16191.
122. Chai JD, Head-Gordon M (2008) Long-range corrected hybrid density functionals with damped atom-atom dispersion corrections. *Phys Chem Chem Phys* 10:6615-6620.
123. Staroverov VN, Scuseria GE, Tao JM, Perdew JP (2003) Comparative assessment of a new nonempirical density functional: Molecules and hydrogen-bonded complexes. *J Chem Phys* 119:12129-12137.
124. Zhao Y, Lynch BJ, Truhlar DG (2004) Development and assessment of a new hybrid density functional model for thermochemical kinetics. *J Phys Chem A* 108:2715-2719.

125. Boese AD, Martin JM (2004) Development of density functionals for thermochemical kinetics. *J Chem Phys* 121:3405-3416.
126. Zhao Y, Lynch BJ, Truhlar DG (2005) Multi-coefficient extrapolated density functional theory for thermochemistry and thermochemical kinetics. *Phys Chem Chem Phys* 7:43-52.
127. Zhao Y, Truhlar DG (2005) Benchmark databases for nonbonded interactions and their use to test density functional theory. *J Chem Theory Comput* 1:415-432.
128. Zhao Y, Truhlar DG (2005) Design of density functionals that are broadly accurate for thermochemistry, thermochemical kinetics, and nonbonded interactions. *J Phys Chem A* 109:5656-5667.
129. Zhao Y, Truhlar DG (2006) Density functional for spectroscopy: No long-range self-interaction error, good performance for Rydberg and charge-transfer states, and better performance on average than B3LYP for ground states. *J Phys Chem A* 110:13126-13130.
130. Zhao Y, Truhlar DG (2008) The M06 suite of density functionals for main group thermochemistry, thermochemical kinetics, noncovalent interactions, excited states, and transition elements: two new functionals and systematic testing of four M06-class functionals and 12 other functionals. *Theo Chem Acc* 120:215-241.
131. Zhao Y, Truhlar DG (2008) Exploring the limit of accuracy of the global hybrid meta density functional for main-group thermochemistry, kinetics, and noncovalent interactions. *J Chem Theory Comput* 4:1849-1868.
132. Peverati R, Truhlar DG (2011) Improving the accuracy of hybrid meta-GGA density functionals by range separation. *J Phys Chem Lett* 2:2810-2817.
133. Tawada Y, Tsuneda T, Yanagisawa S, Yanai T, Hirao K (2004) A long-range-corrected time-dependent density functional theory. *J Chem Phys* 120:8425-8433.
134. Vydrov OA, Scuseria GE (2006) Assessment of a long-range corrected hybrid functional. *J Chem Phys* 125:234109.
135. Vydrov OA, Heyd J, Krukau AV, Scuseria GE (2006) Importance of short-range versus long-range Hartree-Fock exchange for the performance of hybrid density functionals. *J Chem Phys* 125:074106.
136. Vydrov OA, Scuseria GE, Perdew JP (2007) Tests of functionals for systems with fractional electron number. *J Chem Phys* 126:154109.
137. Becke AD (1988) Density-functional exchange-energy approximation with correct asymptotic behavior. *Phys Rev A* 38:3098-3100.
138. Luo S, Zhao Y, Truhlar DG (2011) Validation of electronic structure methods for isomerization reactions of large organic molecules. *Phys Chem Chem Phys* 13:13683-13689.